Manuscript Details

Manuscript number	IBB_2019_1002_R1
Title	Characterization of a biofilm and the pattern outlined by its growth on a granite-built cloister in the Monastery of San Martiño Pinario (Santiago de Compostela, NW Spain)
Article type	Full Length Article

Abstract

The upper zone of the background walls of the processional cloister of the Monastery of San Martiño Pinario (Santiago de Compostela, Galicia, Spain) is affected by a deep green, highly hydrophobic subaerial biofilm. The pattern that the biofilm follows the walls suggests that particular microclimatic conditions induce changes in the biofilm properties. To test this hypothesis, taxonomic and structural identification of the biofilm was carried out by respectively light microscopy and confocal laser scanning microscopy. In addition, the chemical composition was determined by quantification of extracellular polymeric substances in the extracellular matrix of the biofilm, and hydrophobicity was determined by contact angle and water drop penetration time of biofilm and cells. Furthermore, the bioprotective or biodeteriorative role of the biofilm on the cloister is discussed on the basis of the results of stereoscopic microscope observations, X-ray diffraction and attenuated total reflectance-Fourier transform infrared spectroscopy analysis of granite samples from uncolonized areas and from underneath the biofilm. The findings showed that Apatococcus lobatus is the predominant algae in the biofilm. The presence of this alga is favoured by water condensation and it neither damages nor protects the substrate, only causing an aesthetic impact.

Keywords	Apatococcus lobatus; biodeterioration; cultural heritage; extracellular matrix (ECM); hydrophobicity; subaerial biofilm (SAB).
Taxonomy	Biodeterioration, Culture Heritage, Colonization, Microorganism, Damage to Buildings, Stone

Corresponding Author	Patricia Sanmartín
Corresponding Author's Institution	University of Santiago de Compostela (USC)
Order of Authors	Patricia Sanmartín, Federica Villa, Francesca Cappitelli, Sabela Balboa, Rafael Carballeira

Submission Files Included in this PDF

File Name [File Type]

cover letter.docx [Cover Letter]

Response to Reviewers_IBB_2019_1002.docx [Response to Reviewers]

Highlights.docx [Highlights]

Part 1_Manuscript colonization_revised_accepted changes.docx [Manuscript File]

Figure 1.pdf [Figure]

Figure 2.tiff [Figure]

Fig 3_R1.jpg [Figure]

Figure 4.pdf [Figure]

Figure 5.jpg [Figure]

Figure S1.pdf [Figure]

Figure S2.tif [Figure]

Figure S3.tif [Figure]

Figure S4.jpg [Figure]

Table 1_R1.docx [Table]

conflict of interest.docx [Conflict of Interest]

Part 1_Manuscript colonization_FINAL_R1 PATRICIA SM.docx [Supporting File]

Table S1.docx [Supporting File]

Submission Files Not Included in this PDF

File Name [File Type]

video S1.mp4 [Video]

To view all the submission files, including those not included in the PDF, click on the manuscript title on your EVISE Homepage, then click 'Download zip file'.

Santiago de Compostela, Spain. August 8, 2019

Prof. Dr Ji-Dong Gu

Editor in Chief

International Biodeterioration & Biodegradation

Dear Ji-Dong Gu,

I hereby include a manuscript entitled **"Characterization of a biofilm and the pattern outlined by its growth on a granite-built cloister in the Monastery of San Martiño Pinario (Santiago de Compostela, NW Spain)"**, written by myself, F. Villa, F. Cappitelli, S. Balboa, and R. Carballeira to be submitted as a research article for consideration of publication in the Special Issue IBBS2018 of International Biodeterioration & Biodegradation (IBB) journal.

We think the study here presented fits the Aims and Scope of the journal International Biodeterioration & Biodegradation (IBB) and hope it could be considered for publication.

On behalf of my colleagues and myself, I affirm that this paper has not been published before in any form, that it is not under consideration by another journal at the same time as IBB, and that all authors approve of its submission to IBB.

I hope that the editorial board will agree on the interest of this study.

Sincerely yours,

Patricia Sanmartín, on behalf of the authors.

Patricia Sanmartín
Departamento de Edafoloxía e Química Agrícola
Facultade de Farmacia. Pavillón A - Soto. Campus Vida
Universidade de Santiago de Compostela
15782 Santiago de Compostela (A Coruña). SPAIN.
Tel : +34 881814984
https://orcid.org/0000-0002-5733-8833
http://webspersoais.usc.es/persoais/patricia.sanmartin/

Oxford, UK

November 9th, 2019

Professor Ji-Dong Gu
Editor-in-Chief
International Biodeterioration & Biodegradation

We are sending you the revised version of our manuscript entitled **"Characterization of a biofilm and the pattern outlined by its growth on a granite-built cloister in the Monastery of San Martiño Pinario (Santiago de Compostela, NW Spain)"** (Ref: IBB_2019_1002) written by myself, F. Villa, F. Cappitelli, S. Balboa and R. Carballeira. In revising this paper, we have tried to fully address the comments made by the Reviewers via amendments in the text.

We hope the manuscript will now be judged suitable for publication in International Biodeterioration & Biodegradation, and we look forward to hearing from you at your earliest convenience.

Yours sincerely,
Patricia Sanmartín, on behalf of the authors.
Departamento de Edafoloxía e Química Agrícola
Facultade de Farmacia. Pavillón A - Soto. Campus Vida
Universidade de Santiago de Compostela
15782 Santiago de Compostela (A Coruña). Spain
Current address: School of Geography and the Environment, University of Oxford, South Parks Road, Oxford OX1 3QY, UK.

RESPONSES TO THE REVIEWERS' COMMENTS:

Reviewer 1

Conclusions: I think that the conclusions should be broader, not only listing the experimental results.
Response: In agreement with the reviewer suggestion, the conclusions have been extended.

Lines 130-131: Since open porosity is a dimensionless magnitude, expressed as %, the parentheses (v v-1) should be deleted.
Line 136: Change "in the upper three cm" by "in the upper three centimeters"
Line 161, Line 164: "(final concentration, 0.8 mM)" I suppose the authors mean that the concentration is 8 milimoles, if this is the case they should take into account that the SI symbol of unit of amount of substance, mole, is mol, thus, they should be write "(final concentration, 0.8 mmol)". The same in Line 164
Line 173: "Five areas of 20 cm^3" or "Five areas of 20 cm^2"?
Line 205, Line 212: Since 1979, the litre may be written using either an uppercase "L" or a lowercase "l", a decision prompted by the similarity of the lowercase letter "l" to the numeral "1". The American NIST recommends that within the United States "L" be used rather than "l".
Line 227: "three fragments of approx. 2.5 x 1.8 x 0.2 cm^3" should be written "three fragments of approx. 2.5 cm x 1.8 cm x 0.2 cm"
Line 246: (4000 to 400 cm^{-1}) should be written (4000 cm^{-1} to 400 cm^{-1})
Response: Done.

Line 283: What does it mean (2.8 - 4.7 x 5.3 - 18.6 μm)? It should be rewritten in a clearer way.
Line 285-286: What does it mean "The dry weight of the biofilm covering the walls was 0.32 ± 0.07 (0.27 - 0.35) g cm^{-2}"? It should be rewritten in a clearer way. Furthermore, "dry weight" should be changed to "dry weight per unit area"
Response: Rewritten.

Lines 359-362: The paragraph "In the seemingly most hydrophobic samples (1 and 2), the average polysaccharide content was 0.744 and 0.659 $mg/mg_{drybiomass}$ respectively, while the less water-repellent 3 and 4, had a carbohydrate content approximately 3 times lower than their counterparts, 0.185 and

0.229 mg/$mg_{drybiomass}$." Should be rewritten "In the seemingly most hydrophobic samples (1 and 2), the average polysaccharide content was 0.744 mg/$mg_{drybiomass}$ and 0.659 mg/$mg_{drybiomass}$ respectively, while the less water-repellent samples (3 and 4) had a carbohydrate content of 0.185 mg/$mg_{drybiomass}$ and 0.229 mg/$mg_{drybiomass}$ which are approximately 3 times lower than their counterparts.
Table 1: The estimated uncertainty in the content of polysaccharides and proteins, expressed in terms of SD, should be rounded to 2 significant figures.

Response: Done.

Reviewer 2

Regarding the observation at the CLSM: it is not so clear that the 'cells occurred in densely packed EPS-glyconjugates aggregates…' as stated in lines 279-280. In fig. 2 the red signal doesn't seem highly spread in the microbial community but only limited to part of it. Moreover, the caption of fig. 2 is not so clear: what do you mean with 'panel A'? which type of biofilm is the figure referring to? The biofilms in the two pictures are from different places? Are they hydrophobic or hydrophilic biofilms? Explain better in the caption and in the text all these points.

Response: In agreement with the reviewer suggestions, this part of the manuscript has been clarified.

Figure 3: the scale bar is reported only in C. Image in B is a magnification of image in A? the image A is obtained with a digital camera? Or with the Dino-Lite?

Response: In agreement with the reviewer suggestions, this part of the manuscript has been clarified.

Reviewer 3

136 - I think you have an extra space before "upper"
260 - The same with "3 %"
282, 290, 295 - You write "alga" but I think the plural "algae" is the correct one in these places
303 - "60-km" , don't think it needs the "-" , your choice.

Response: Done.

305 - "The algae preferred areas..." If you are referring to referring to T. umbrina specifically, then I guess "This alga" is more correct, if you are referring to all algae that were growing, then it's ok as it is. However, it is not very clear.

Response: In agreement with the reviewer suggestions, this part of the manuscript has been clarified.

Highlights

- *Apatococcus lobatus* is the predominant species in the algal biofilm

- Microclimate affects the greening pattern of the hydrophobic algal biofilm

- Condensation is assumed to be a key factor in algal growth

- The biofilm does not protect or deteriorate the stone substrate

- The presence of *Apatococcus lobatus* only has an aesthetic impact

Characterization of a biofilm and the pattern outlined by its growth on a granite-built cloister in the Monastery of San Martiño Pinario (Santiago de Compostela, NW Spain)

P. Sanmartín [1*], F. Villa [2], F. Cappitelli [2], S. Balboa [3], R. Carballeira [1,4]

1. Departamento de Edafoloxía e Química Agrícola. Facultade de Farmacia. Universidade de Santiago de Compostela, 15782 - Santiago de Compostela, Spain.
2. Dipartimento di Scienze per gli Alimenti, la Nutrizione e l'Ambiente (DeFENS). Università degli Studi di Milano, Via Celoria 2, 20133 - Milano, Italy.
3. Departamento de Microbioloxía e Parasitoloxía, CIBUS-Facultade de Bioloxía and Instituto de Acuicultura, Universidade de Santiago de Compostela, 15782 - Santiago de Compostela, Spain.
4. Centro de Investigacións Científicas Avanzadas (CICA), Facultade de Ciencias, Universidade da Coruña, A Coruña, Spain.

*Corresponding author: Patricia Sanmartín
Telephone: +34 881814984 Fax: +34 881 815106
E-mail address: patricia.sanmartin@usc.es

Full postal address: Patricia Sanmartín Sánchez
Departamento de Edafoloxía e Química Agrícola
Facultade de Farmacia. Pavillón A - Soto. Campus Vida
Universidade de Santiago de Compostela
15782 Santiago de Compostela, A Coruña. Spain

Abstract

The upper zone of the background walls of the processional cloister of the Monastery of San Martiño Pinario (Santiago de Compostela, Galicia, Spain) is affected by a deep green, highly hydrophobic subaerial biofilm. The pattern that the biofilm follows the walls suggests that particular microclimatic conditions induce changes in the biofilm properties. To test this hypothesis, taxonomic and structural identification of the biofilm was carried out by respectively light microscopy and confocal laser scanning microscopy. In addition, the chemical composition was determined by quantification of extracellular polymeric substances in the extracellular matrix of the biofilm, and hydrophobicity was determined by contact angle and water drop penetration time of biofilm and cells. Furthermore, the bioprotective or biodeteriorative role of the biofilm on the cloister is discussed on the basis of the results of stereoscopic microscope observations, X-ray diffraction and attenuated total reflectance-Fourier transform infrared spectroscopy analysis of granite samples from uncolonized areas and from underneath the biofilm. The findings showed that *Apatococcus lobatus* is the predominant algae in the biofilm. The presence of this alga is favoured by water condensation and it neither damages nor protects the substrate, only causing an aesthetic impact.

Keywords: *Apatococcus lobatus*; biodeterioration; cultural heritage; extracellular matrix (ECM); hydrophobicity; subaerial biofilm (SAB).

1. Introduction

The patterns and drivers of biological colonization on buildings, which is closely related to the bioreceptivity concept (Guillite, 1995), is an interesting and topical field of study. Although bioreceptivity is determined by intrinsic characteristics of the substrate such as roughness and porosity (Guillite, 1995; Miller et al., 2012; Vázquez-Nion et al., 2018; Sanmartín et al., 2019), other factors such as the slope angle, surface geometry and degree of shading (Viles and Ahmad, 2016), presence of synthetic polymers (Cappitelli et al., 2004) and also surface colour (Gambino and Sanmartín et al., 2019) have been found to influence phototrophic colonization.

Green algae (chlorophytes) and cyanobacteria (cyanophytes) colonize stonework whenever moisture, light, temperature and nutrient conditions are favourable. According to Liu et al. (2018), stone porosity, temperature and available water/moisture are the critical factors triggering biological colonization on stone surfaces. The duration of damp periods and cooler temperatures strongly affect phototrophic biofilm formation (Ortega-Calvo et al., 1995; Nugari et al., 2009). Under tropical climate conditions, intense sunlight, together with natural rainwater, also strongly promotes colonization (Zhang et al., 2019). Phototrophic biofilms usually occur on damp patches (caused by rainfall) on walls (Gorbushina, 2007; Charola et al., 2008). In France and Germany, north- and west-facing walls are more affected by precipitation (Barberousse et al., 2007), while in the city of Oxford (UK), south- and west-facing walls are more strongly affected (Thornbush, 2014). Heavy precipitation can also cause microorganisms to be removed from the walls. Indeed, in order to measure urban greening in Oxford, Thornbush (2013) selected the north-facing sides because these are usually most prone to presence of phototrophs.

Light is also an important factor controlling phototrophic growth. The ubiquitous green alga *Trentepohlia* sp. grows in very humid areas. It often occurs on concrete, which is porous and retains much water, in areas with sufficient light, although not direct sunlight (Ariño and Saiz-Jimenez, 1996). In poorly lit areas, cyanobacteria are more competitive than algae, covering zones where lichens, which need dry substrates with abundant light, are almost totally absent (Ariño and Saiz-Jimenez, 1996). The phototrophic community may be mainly composed of eukaryotic algae or cyanobacteria, depending on the light exposure. This is the case of the Khmer temples in Angkor (Cambodia), where the initial pioneer community is primarily composed of a reddish biofilm of a green alga that occurs in dry, shady conditions, whereas cyanobacteria prevail in dry, sunny conditions (Caneva et al., 2015).

A number of papers report that phototrophic microorganisms can cause damage to different types of stone and that deterioration is primarily due to the physical features of the stone surface, microclimate and environmental conditions and secondarily to the lithotype (as reviewed in Macedo et al., 2009). By contrast, some papers claim that lichens can protect stone from damage as in the ‘Casa Lis’, in Salamanca, Spain, which

is built from highly porous Villamayor sandstone (Grondona et al., 1997). Other sessile phototrophic microorganisms can act as protective agents for stone materials (Cutler et al., 2013; Pinna, 2017).

The monastery of San Martiño Pinario (UTM 29T X 537220, Y 4747793; Datum ETRS89) is one of the most emblematic buildings in Galician culture and the second most important historical building (after the Cathedral) in the city of Santiago de Compostela (UNESCO World Heritage City since 1985, capital of Galicia, north-western Spain). The processional cloister, built between 1633 and 1747 (for more information, see Sanmartín et al., this issue), has a deep green, highly hydrophobic subaerial biofilm in the upper zone of the background walls in areas protected from rainfall. This biofilm, reported to be present at least for 50 years, was characterized in detail in the present study, and the taxonomic identification, architecture and extracellular matrix are reported. Its bioprotective or biodeteriorative role was also considered by comparing results obtained by stereoscopic microscope, X-ray diffraction and Fourier Transform infrared analysis of granite samples from uncolonized areas and from underneath the biofilm.

2. Materials and methods

2.1. Colonization pattern and masonry description

The biofilm occurs at a height of about 3 meters, sheltered from rain and direct sunlight and mainly concentrated on north- and west-facing walls (Figure 1). The biofilm is highly water repellent (hydrophobic) (Video 1, supplementary material). The biofilm is present on the surface of the granite ashlars and absent from the joint mortar. The background walls of the cloister are formed by granite masonry, a migmatic granitoid with preferred orientation of biotite and hypidiomorphic granular texture (Rivas et al., 2000). Its open porosity (following RILEM 1980), closely related to the water saturation capacity, is 4.6% (Rivas et al., 2000), which is high in comparison with the open porosity values of 0.1 to 2% usually observed in sound granitic rocks (UNE-EN 1936:1999; Silva et al., 2019). The porosity of granite increases with the inter- and intra-granular fissures and a well-connected network of fissures, as well as the presence of clay minerals such as chlorite, kaolinite and vermiculite. According to Rivas (1997), the ashlar rock in the processional cloister of the Monastery of San Martiño Pinario displays a high degree of fissuring, especially in the upper three centimetres, while its modal composition comprises quartz (49%), plagioclase (12%), alkaline feldspar (microcline-9%), muscovite (16%) and biotite (partly chloritized-12%), as main minerals, and kaolinite and vermiculite in trace amounts (<3%).

The joint mortar was analysed in the present study by X-ray diffraction (XRD), in a PW1710 Philips diffractometer equipped with a PW1820/00 goniometer and an Enraf Nonius FR590 generator operating at 40 kV and 30 mA. The X-rays were obtained with CuKα-radiation (λ = 1.5406 Å), and the XRD diffractogram patterns were acquired in

the angular range of $2<2\theta<65$ with a step size of 0.02° and a measuring time of 2 s per step. Identification of the minerals was made by comparison with the ICSD and COD databases.

The pH of granite and joint mortar was measured with pH-Universal indicator strips (MERK) after contact for 60 ± 5 seconds, according to the American Standard ASTM F710.

2.2. Biofilm architecture

Biofilm samples were collected using the non-invasive method with adhesive tape strips. Strips were gently applied to the stone surface and then placed on sterile glass microscope slides and transported in a box to the laboratory. The adhesive tape strips were then immediately analysed by confocal laser scanning microscopy (CLSM).

Confocal images were collected using a Nikon A1 laser scanning confocal microscope and a 20x/0.75NA (WD 1 mm) Plan Apo λ objective. Fluorescence was excited and collected using different combinations of the following laser lines and emission parameters: i) autofluorescence from photosynthetic pigments was viewed in the blue channel using the 633 nm line of an Ar/HeNe laser in the emission range of 650 to 750 nm; ii) EPS were labelled with the lectin Concanavalin-A- Texas red (Molecular Probes, Inc., Eugene, OR, USA) (final concentration, 0.8 mmol) and observed in the red channel (excitation at 561 nm line, and emission at 590 to 630 nm); iii) chemotrophs were visualized in green (excitation at 488 nm line, and emission at 500 to 550 nm) after staining with Syto9 (final concentration, 50 μmol).

CLSM was used in reflectance mode with the 488 nm argon line for relief imaging of specimens. Captured images were analysed with NIS-Elements software (Nikon) for 3D reconstruction of biofilms.

2.3. Taxonomic identification

The subaerial biofilm was first examined on site with a Dino-Lite AM3113T digital handheld microscope with DinoXcope Imaging Software. Subsequently, ten micro-samples of biofilm were removed from several areas of the background walls of the processional cloister with the aid of scalpel and placed sterile plastic tubes, for identification by light microscopy. Five areas of 20 cm^2 were scraped from the walls for biomass determination. The micro-samples were examined under a stereoscopic microscope (Nikon Eclipse E600, Tokyo, Japan) equipped with an E-Plan x40 objective (N.A. 0.65) and differential interference contrast (Nomarski) optics. Light microscopy photographs were taken with an AxioCam ICc5 Zeiss digital camera. Taxonomic determinations were based on the morphometry and reproduction of the species in culture, following the taxonomic criteria of Ettl and Gäertner (1995), Rifón-Lastra (2000), Rifón-Lastra and Noguerol-Seoane (2001) and Rindi and Guiry (2004).

2.4. Wetting characterization by contact angle analysis

A Drop Shape Analyzer DSA 100 (Krüss GmbH, Hamburg, Germany) was used for water repellency measurements: a droplet of distilled water (10 μL) was deposited onto the target surface and the water-surface contact angle was immediately measured. No fewer than 5 measurements were made on different zones of the target surface at 25 °C. The contact angle was measured on digital microphotographs with Image J2 software (Rueden et al. 2017). The water drop penetration time (WDPT) test was conducted according to Leelamanie et al. (2008).

During the first observations (section 2.3.), a simple on-site test with a wash bottle indicated that some parts of the biofilm were more hydrophobic than others. For this reason and for global characterization of the biofilm, measurements were made in biofilm samples with greater and lower degrees of water repellency. In addition, and for comparative purposes, measurements were made on uncolonized granite, granite underneath the biofilm and algal cells, after extracting the extracellular matrix.

2.5. Extracellular polymeric substances (EPS)

Four areas (each 18 cm^2) of the colonized upper zone of the background walls of the cloister were scraped to remove the biofilm. The cells of the exopolymeric matrix (EPS) were then separated and the main components were identified: carbohydrates (polysaccharides) and proteins.

As in section 2.4., EPS analysis was performed in samples taken from the most hydrophobic areas (samples 1 and 2) and from the less hydrophobic areas (samples 3 and 4).

Approximately 1.5 g of biofilm sample was obtained in each area and split into three subsamples. The EPS extraction was performed following Villa et al. (2015), with a slight modification. Briefly, 0.04 g of each subsample was resuspended in 2 mL 2% ethylenediaminetetraacetic acid by vortexing and sonication in a bath (45 kHz) for 10 min. Samples were vortexed again and shaken at 300 rpm for 3 h at 4ºC. To separate the cell debris from the supernatant containing the EPS, the samples were filtered through 0.22 μm nitrocellulose membranes (Millipore). The EPS was then precipitated overnight in two volumes of chilled ethanol at -20ºC, centrifuged at 13000 rpm for 30 min at 4ºC and washed twice with 95% ethanol. Samples were then air-dried and resuspended in 380 μL of M9 mineral medium. Each subsample was then diluted in distilled water, and the carbohydrate content of the EPS was measured by the phenol-sulfuric method, with glucose as standard. The amount of carbohydrate or polysaccharide content was expressed as the mean ratio relative to the dry biomass, following Villa et al. (2012). The protein content was measured following the Bradford assay (Bradford, 1976) in microtitre plates.

2.6. Analysis of the impact of biofilm on the granite

In addition to the obvious aesthetic biodeterioration, any possible physical and chemical alteration of the granite building material caused by the biofilm was determined by analysis in a stereoscopic microscope (Nikon Model SMZ1500) equipped with a Digital Camera (Nikon DXM 1200) and a digital image capture software (Nikon ACT-1). Fragments of samples with subaerial biofilm were examined, focusing attention on the appearance of the granite under the biofilm. Fragments without subaerial biofilm were also examined for comparative purposes.

Furthermore, three fragments of approx. 2.5 cm x 1.8 cm x 0.2 cm of each of the colonized and uncolonized areas were taken for comparison of the changes triggered by the biofilm in the mineralogical composition and compositional features of granite building material. In the three colonized samples, the biofilm was carefully removed from the stone surface with the aid of a soft brush, and granite samples were obtained from underneath the biofilm (U1-U3) for analysis. The samples were compared with three reference granite samples from adjacent uncolonized areas (N1-N3). The six samples were crushed separately into small particles and ground to a very fine powder (<50 μm the diameter of particle). Each sample was then divided into two equal parts: one for X-ray diffraction study of mineralogical composition and another for attenuated total reflectance-Fourier transform infrared spectroscopy analysis for identification of the components.

For X-ray diffraction (XRD), the same device and conditions described in Section 2.1. were used. The granite samples were turned over to obtain profiles optimal peak for analysis, as well as minimize the effect of preferential orientation.

Attenuated total reflectance-Fourier transform infrared spectroscopy (ATR-FTIR) was carried out in a Varian 670-IR spectrometer (Varian Inc., Santa Clara, CA) equipped with an ATR device with a single-reflection diamond crystal (Pike GladiATR, Madison, WI). The spectra were obtained with an angle of incidence for the infrared beam through the diamond crystal of 45°, in the spectral range of the medium (4000 cm^{-1} to 400 cm^{-1}) and a resolution of 4 cm^{-1}.

2.7. Statistical analysis

The quantities of both EPS components (polysaccharides and proteins) were statistically compared using a Kruskal-Wallis test with Conover-Iman multiple pairwise comparisons at a significance level of 95 % ($\alpha = 0.05$) and Bonferroni correction. Pearson correlation coefficients (R) were calculated for both EPS components and the measured contact angles, and t-test, with a significance level of 95 % ($\alpha = 0.05$). All statistical analyses were performed using XLSTAT 2019 software.

3. Results and discussion

3.1. Characterization of the biofilm and the pattern outlined

The presence of biofilm is visually homogeneous over the surface of the granite ashlars surface (pH 6 to 7). By contrast, the joint mortar is not colonized. It is a lime mortar of pH 8 to 9, with calcite ($CaCO_3$, 23%) and gypsum ($CaSO_4$ $2H_2O$, 3%) as dominant phase, and granite sand with a mineral composition very similar to the ashlars, indicating that crushed quarry material was probably reused as aggregate for the mortar.

Representative images of the biofilm obtained from the granite surface are shown in Figure 2. The images correspond to the Maximum Intensity Projection (MIP) 3D reconstructions obtained from confocal images series with the dedicated NIS-Elements software. The fluorescent signals in Figure 2 detected cells in the biofilms. A patchy distribution of small cell aggregates can be seen to follow the topography of the surfaces.

Overall, the predominance of phototrophic communities (blue signal) was characterised by coccoid structures assembled in clusters, while the Syto9 stain did not reveal an extensive chemotrophic microbial community. However, these communities were highly developed in zones with weak or absent photosynthetic pigment fluorescence. The red signal, derived from the lectin-binding dye Con A, revealed the presence of extracellular glycoconjugates (i.e. polysaccharides, including those covalently linked to proteins and/or lipids) covering the granite surfaces and partly overlapping the blue signal of phototrophs. Overall, the microscopic studies revealed the following: i) the granite substrate is colonized by a monolayer of cells growing in small clusters that follow rock fissures and cracks; ii) phototrophs comprised the largest proportion of the biofilm community in all specimens analyzed; and iii) microbial cells occurred in densely packed aggregates surrounded by the EPS matrix.

Taxonomic identification of the biofilm showed that *Apatococcus lobatus* (Chodat) J.B.Petersen (Chlorophyta) was the predominant species, with some of the algae appearing partially lichenized. *A. lobatus* cells are 2.8 - 4.7 μm wide and 5.3 - 18.6 μm long, macroscopically form sarcinoid aggregates with a bright green powdery consistency and up to 100 μm thick (Figure 3). The dry weight per unit area of the biofilm covering the walls was 0.32 ± 0.07 g cm^{-2}, and the moisture content of the fresh biofilm was 65 %.

Apatococcus lobatus is a widely documented, cosmopolitan species in subaerial environments and niches, including anthropogenic constructions (Ettl and Gärtner, 1995; Rifón-Lastra, 2000; Rifón-Lastra and Noguerol-Seoane, 2001; Barberousse et al., 2006). It is a species of green algae with mixotrophic metabolism with generally low growth rates but which increase greatly with organic inputs (Gustavs et al., 2016). This may be an important adaptive advantage in the colonization of acid subaerial habitats (such as granite walls) where bacterial activity is generally lower. This species is one of

the most abundant algae in temperate Europe, forming robust biofilms on tree bark and building surfaces (Gustavs et al., 2011). *A. lobatus* has previously been observed colonizing granite outcrops in the Ukraine valleys (Mikhailyuk, 2013).

The presence of *A. lobatus* in subaerial environments protected from rainfall is probably related to its high resistance to desiccation, e.g. due to thickening of the cell wall, which waterproofs the cells and prevents dehydration (Wurtz, 1944), as well as explaining the strong hydrophobic character of the biofilm observed during the study (Figure 3 and Video 1, supplementary material). Similarly, biofilms collected across an altitude range from sea level to around 900 m, along the coast of Lazio (Italy) to 60 km inland, showed a dominant presence of the filamentous terrestrial green alga *Trentepohlia umbrina* (Kützing) Bornet (Bartoli et al., 2019). This alga was found to prefer areas of low relative humidity (RH) on exposed north-facing vertical surfaces. This dominance was explained by the higher nocturnal condensation typical of coastal areas.

Galicia has an oceanic climate with high atmospheric humidity caused by high rainfall and mild temperatures throughout the year (Martínez-Cortizas and Pérez-Alberti, 1999). According to data for the last ten years (2009-2019), the relative humidity (RH) in Santiago de Compostela is between 77 and 85% (www.meteogalicia.gal). A previous study (Bertsch, 1966) investigated the effect of desiccation of *A. lobatus* induced by decreasing air humidity. Although carbon assimilation was reported to be highest at or above 97–98% RH, half of the maximum carbon dioxide-uptake still took place at 90% RH, with the lowest level of carbon assimilation occurring at 68% RH (Bertsch, 1966). These data clearly showed that moisture favoured carbon dioxide uptake by *A. lobatus*, while water had an unfavourable effect, and also showed that average humidity in Santiago de Compostela is not sufficient for the optimal growth of the green alga.

Microclimatic effects affect the pattern outlined by the biofilm growth. First, north- and west-facing walls are clearly more prone to algal colonization growth, which is explained by the fact that algae are transported by wind as spores (Barberousse et al., 2007) as well as by wind-driven precipitation and by the fact that in Galicia the prevailing wind direction is west or north-west (www.meteogalicia.gal; www.meteoblue.com). Second, the biofilm only appears in the areas of the wall shaded from direct sunlight, and the undulating pattern of colonization is explained by the sunlight passing through the central arches of the courtyard (Figure S1). As Barberousse et al. (2007) explain, a gradient of temperature on a facade, with one area cooler than another warmed by the sun, may result in condensation of atmospheric humidity in the first area, favouring algal growth in the cool area. In recent years, various different masonry surfaces have been observed to be covered with algae. In the German town of Rostock, most buildings were constructed in the 1970s using concrete and were renovated in 1993 by adding insulation and artificial resin plaster to the surface. Shortly afterwards, these coatings became almost totally covered by green microalgae, mainly on the north and west sides, especially in areas not exposed to full solar radiation (Häubner et al., 2006). In a recent paper by Steffgen (2019), the phototrophic growth

was related to improved thermal insulation of buildings and the accumulation of condensation was considered of decisive importance.

3.2. Biofilm hydrophobicity

According to the categories of water repellency assigned by Leelamanie et al. (2008), both biofilm samples, seemingly more and less hydrophobic, were found to be extremely repellent to the water, with the time taken for the complete penetration of the water drop of more than an hour and water contact angles of 133.5º ± 3.5º and 119.4º ± 4.8º, respectively (Figure 4). The contact angle could not be measured on uncolonized granite as the drop was absorbed immediately upon falling. The water drop penetration time (WDPT) was less than 0.2 s, corresponding to instantaneous penetration and non-repellent character. The hydrophobicity of the rock where the biofilm was formed was still notable after biofilm removal (contact angle of 101.9º □ 4.9º), although the WDPT value was greatly reduced, by up to 60-600 s, considered strongly repellent (Figure 4). The contact angle of the samples after extraction of the EPS was drastically reduced, to 85.6º ± 2.7º, and the WDPT values of the cells was as low as one second, indicating that they were not water repellent. These values were very similar to those of the nitrocellulose membrane where the cells were deposited: 58.7º ± 1.0º and the same category in the WDPT (Figure 4).

The polysaccharide and protein contents of the biofilm matrix are shown in Table 1. The polysaccharide content of the four samples varied greatly depending on the sampling area, with significant differences in 1 and 2, relative to 3 and 4 (Box plots of the EPS components are presented as supplementary information, Figure S2). In the seemingly most hydrophobic samples (1 and 2), the average polysaccharide content was 0.74 mg/mg $_{dry\ biomass}$ and 0.66 mg/mg $_{dry\ biomass}$ respectively, while the less water-repellent samples (3 and 4) had a carbohydrate content of 0.18 mg/mg $_{dry\ biomass}$ and 0.23 mg/mg $_{dry\ biomass}$, i.e. approximately 3 times lower than their counterparts. On the contrary, the protein content of the four samples did not differ, with average values of 0.28, 0.28, 0.29 and 0.29 μg/mg $_{dry\ biomass}$. Thus, almost three quarters of the EPS were polysaccharides in samples 1 and 2, while in samples 3 and 4, polysaccharides only made up approximately 40-45% of the total EPS (Table 1). Furthermore, the contact angle values and polysaccharides content were highly correlated ($R = 0.8312$, $t = 0.912$, p-value < 0.0001), while the correlation with proteins was low ($R = 0.2541$, $t = -0.504$, p-value = 0.095). The correlations between EPS components and the contact angle values are presented as supplementary information, Figure S3).

Biofilms can protect masonry materials, also depending on the hydrophilic or hydrophobic features of their matrices. The hydrophilic character of extracellular polymeric substances (EPS) is linked to functional groups of hydrophilic nature such as hydroxyl and carboxyl, as well as phosphate, amine and sulphate, while the hydrophobic character is associated with non-polar regions, such as aromatic and aliphatic regions in proteins and hydrophobic regions in O-methyl/acetyl polysaccharides (Moran, 2009). Extracellular polysaccharides are critical in desiccation

tolerance of both cyanobacteria and green algae (Knowles and Castenholz, 2008). Thus, increasing the amount of exopolysaccharides may be a compensatory measure to enhance the efficiency of photosynthesis.

3.3. Role of biofilm on granite conservation

Stereoscopic observations (Figure 5) were consistent with the previous CLSM observations described in section 3.1. Biofilm seems to cover the granite surface by forming aggregates, sometimes surrounding the mineral grains. These grains remained unattached on the surface, and they were observed in the images of the uncolonized granite, with a very sandy surface and visible oxidation of Fe in biotites.

X-ray diffraction (XRD) analysis showed that, relative to the uncolonized granite, the biofilm did not cause any mineralogical changes (Table S1). The mineral composition was very similar in the six samples and semiquantitative measurements coincided with those reported by Rivas (1997). The presence of gypsum in samples N1 and N2 was the only remarkable feature in the XRD analysis (Table S1). Given that gypsum is present in the joint mortar (section 3.1), the most likely hypothesis is that it originates from the mortar and moved to the ashlar.

Analysis of the samples by ATR-FTIR spectroscopy confirmed the lack of mineralogical transformation of the granite (Figure S4). The same bands were seen in all the samples and are representative of the minerals that form granitic rocks, such as the abundant characteristic bands of silicates corresponding to Si-O (quartz), Si-O-Si (quartz), and Si-O-Al (feldspar) in the range 400 – 1100 cm^{-1} (Socrates, 2001; Pozo-Antonio et al., 2018). Only three slightly different signals appeared in the infrared spectra, and none were related to alteration of the granite underneath the biofilm:
(1) The peak with a shoulder at around 1030–1100cm^{-1}, characteristic of silicates and that corresponds to asymmetrical stretching vibration of Si–O (Socrates, 2001; Pozo-Antonio et al., 2018), was present in all the samples. The shoulder, however, was further accentuated in the two samples taken from uncolonized areas N1 and N2, probably by the sum with the peak assigned to gypsum at 1120 cm^{-1} (Socrates, 2001), the only mineral present in these two samples, Table S1). The shoulder disappeared in the samples from under the biofilm (U1-U3) probably by the overlap of the peak with the band at 1040 cm^{-1} corresponding to polysaccharides (Houari et al., 2013) remaining after removal of the biofilm by brushing (section 2.6). The latter is also consistent with the results obtained in the contact angle study (section 3.2).
(2) The weak band at 1630 cm^{-1} that appeared in the uncolonized samples N1 and N2 and that did not appear in the other samples, may be attributed to an organic matter deposit (Madejová and Komadel, 2001), rather than to kaolinite, also associated with this peak but not observed in the X-ray diffraction analysis of either samples (Table S1).
(3) The vibrational band assigned to gypsum at 674 cm^{-1} (Socrates, 2001) only appeared in samples N1 and N2 containing the mineral (Table S1).

Green algae colonizing stone surfaces may represent a major problem for the conservation of heritage monuments, and in the last decade evaluation of whether the algal biofilm is causing damage, is neutral or protects the stone substrate has become mandatory (Vojtková, 2017; Pinna, 2017). Several control methods are now available (Pfendler et al., 2018) and can be applied when biodeterioration is demonstrated.

Salt crystal formation, a major cause of stone deterioration, is favoured by water movement in the pores. A hydrophobic layer on the external surface of the wall, which alters the original wettability of that building material, can lead to humidity that inhibits salt crystal formation (Polson et al., 2002). Indeed, it may act as a natural waterproofing agent on the building, possibly preventing the entry of water. Other types of damage that are potentially prevented or reduced include freeze-thaw damage, salt shattering and mineral dissolution. On the other hand, if the water comes from the walls (e.g. by capillary forces or excess condensation from within the building), it is equally possible that this water could be retained behind the biofilm and cause damage. In the Monastery of San Martiño Pinario, these two situations are apparently well balanced and the biofilm has caused neither deterioration nor protection for at least 50 years.

4. Conclusions

The highly hydrophobic subaerial biofilm in the processional cloister of the Monastery of San Martiño Pinario is mainly formed by *Apatococcus lobatus* (Chodat) J.B.Petersen (Chlorophyta). The study findings showed that the biological growth, promoted by condensation, does not damage or protect the substrate. Indeed, the *A. lobatus* biofilm only has an aesthetic impact on the Monastery walls. On the basis of these results and in view of the future maintenance and conservation of the Monastery building, we recommend that the existing biofilm should not be removed, because it is an interesting case study of a subaerial biofilm and can also be considered part of the cultural heritage in this building. Furthermore, this recommendation is consistent with the 'minimal intervention' concept, i.e. that intervention during heritage conservation activities should be kept to an absolute minimum.

Acknowledgements

This work was financially supported by Xunta de Galicia (grants POS-B/2016/030 and ED431C 2018/32). We thank Carlos Álvarez Varela, dean of the Monastery of San Martiño Pinario, and Eva Varela Rodríguez, secretary of the Seminario Mayor, for permission to conduct research in the Monastery and for their valuable assistance. The authors also thank Prof. Carmen Álvarez-Lorenzo (Universidade de Santiago de Compostela, Spain) for assistance with contact angle measurements.

References

Ariño, X., Saiz-Jimenez, C., 1996. Colonization and deterioration processes in Roman mortars by cyanobacteria, algae and lichens. Aerobiologia 12(1), 9–18.

ASTM International, 2008. F710-08 Standard Practice for Preparing Concrete Floors to Receive Resilient Flooring.

Barberousse, H., Tell, G., Yéprémian, C., Couté, A., 2006. Diversity of algae and cyanobacteria growing on buildings facades in France. Algological Studies 120, 81-105.

Barberousse, H., Ruot, B., Yéprémian, C., Boulon, G., 2007. An assessment of façade coatings against colonisation by aerial algae and cyanobacteria. Building and Environment 42(7), 2555–2561.

Bartoli, F., Ellwood, N.T.W., Bruno, L., Ceschin, S., Rugnini, L., Caneva, G., 2019. Ecological and taxonomic characterisation of *Trentepohlia umbrina* (Kützing) Bornet growing on stone surfaces in Lazio (Italy). Annals of Microbiology, in press.

Bertsch, A., 1966. CO_2-Exchange and water relations in the aerophillic green-alga *Apatococcus lobatus*. Planta 70(1), 46-72.

Bradford, M.M., 1976. A rapid and sensitive method for the quantitation of microgram quantities of protein utilizing the principle of protein-dye binding. Analytical Biochemistry 72, 248–254.

Caneva, G., Bartoli, F. Ceschin, S., Salvadori, O., Futagami, Y., Salvati, L., 2015. Exploring ecological relationships in the biodeterioration patterns of Angkor temples (Cambodia) along a forest canopy gradient. Journal of Cultural Heritage 16(5), 728-735.

Cappitelli, F., Zanardini, E., Sorlini, C., 2004. The biodeterioration of synthetic resins used in conservation. Macromolecular Bioscience 4(4), 399-406.

Charola, A.E., Delgado, R.J., Vale, A.M., 2008. Disfiguring biocolonization patterns after the application of water repellents. Restoration of Buildings and Monuments 14(5), 365–372.

Cutler, N.A., Viles, H.A., Ahmad, S., McCabe, S., Smith, B.J., 2013. Algal 'greening' and the conservation of stone heritage structures. Science of the Total Environment 442, 152–164.

Ettl, H., Gärtner, G., 1995. Syllabus der Boden-. Luft- und Flechtenalgen. pp. i-vii. 1-721. Stuttgart: Gustav Fischer.

Gambino, M., Sanmartín, P., Longoni, M., Villa, F., Mitchell, R., Cappitelli, F., 2019. Surface colour: an overlooked aspect in the study of cyanobacterial biofilm formation. Science of the Total Environment 659, 342-353.

Grondona, I., Monte, E., Rives, V., Vicente, M.A., 1997. Lichenized association between *Septonema tormes* sp. nov., a coccoid cyanobacterium, and a green alga with an unforeseen biopreservation effect of Villamayor sandstone at 'Casa Lis' of Salamanca, Spain. Mycological Research 101(12), 1489-1495.

Gorbushina, A.A., 2007. Life on the rocks. Environmental Microbiology 9, 1613–1631.

Guillitte, O., 1995. Bioreceptivity: a new concept for building ecology studies. Science of the Total Environment 167(1-3), 215-220.

Gustavs, L., Görs, M., Karsten, U., 2011. Polyol patterns in biofilm-forming aeroterrestrial green algae (Trebouxiophyceae, Chlorophyta). Journal of Phycology 47(3), 533-537.

Gustavs, L., Schumann, R., Karsten, U., Lorenz M., 2016. Mixotrophy in the terrestrial green alga *Apatococcus lobatus* (Trebouxiophyceae, Chlorophyta). Journal of Phycology 52, 311–314.

Häubner, N., Schumann, R., Karsten, U., 2006. Aeroterrestrial microalgae growing in biofilms on facades-response to temperature and water stress. Microbial Ecology 51(3), 285-93.

Houari, A., Seyer, D., Kecili, K., Heim, V., Di Martino, P., 2013. Kinetic development of biofilm on NF membranes at the Méry-sur-Oise plant, France. Biofouling 29, 109–118.

Knowles, E.J., Castenholz, R.W., 2008. Effect of exogenous extracellular polysaccharides on the desiccation and freezing tolerance of rock-inhabiting phototrophic microorganisms. FEMS Microbiology Ecology 66(2), 261-270.

Leelamanie, D.A.L., Karube, J., Yoshida, A., 2008. Characterizing water repellency indices: contact angle and water drop penetration time of hydrophobized sand. Soil Science and Plant Nutrition 54, 179-187.

Liu, X., Meng, H., Wang, Y., Katayama, Y., Gu, J.-D., 2018. Water is the critical factor to establishment biological and stability of Angkor temple sandstone in Southeast Asia. International Biodeterioration and Biodegradation 133, 9-16.

Macedo, M.F., Miller, A.Z., Dionísio, A., Saiz-Jimenez, C., 2009. Biodiversity of cyanobacteria and green algae on monuments in the Mediterranean Basin: an overview. Microbiology 155 (11), 3476-3490.

Madejová, J., Komadel, P., 2001. Baseline studies of the clay minerals society source clays: infrared methods. Clays and Clay Minerals 49(5), 410–432.

Mikhailyuk, T.I., 2013. Terrestrial algae from the granite outcrops of river valleys of the Ukraine. International journal on algae 15(4), 311-330.

Miller, A.Z., Sanmartín, P., Pereira-Pardo, L., Saiz-Jimenez, C., Dionísio, A., Macedo, M.F., Prieto, B., 2012. Bioreceptivity of building stones: a review. Science of the Total Environment 426, 1–12.

Moran, A.P., 2009. Microbial Glycobiology: Structures, Relevance and Applications. Elsevier, Oxford.

Martínez-Cortizas, A., Pérez-Alberti, A. (Eds.), 1999. Atlas climático de Galicia. Consellería de Medioambiente, Xunta de Galicia, 207p.

Nugari, M.P., Pietrini, A.M., Caneva, G., Imperi, F., Visca, P., 2009. Biodeterioration of mural paintings in a rocky habitat: the Crypt of the Original Sin (Matera, Italy). International Biodeterioration and Biodegradation 63, 705-711.

Ortega-Calvo, J.J., Ariño, X., Hernandez-Marine, M., Saiz-Jimenez, C., 1995. Factors affecting the weathering and colonization of monuments by phototrophic microorganisms. Science of the Total Environment 167, 329-341.

Pfendler, S., Munch, T., Bousta, F., Alaoui-Sosse, L., Aleya, L., Alaoui-Sossé, B., 2018. Bleaching of biofilm-forming algae induced by UV-C treatment: a preliminary study on chlorophyll degradation and its optimization for an application on cultural heritage. Environmental Science and Pollution Research 25(14), 14097-14105.

Pinna, D., 2017. Coping with biological growth on stone heritage objects: methods, products, applications, and perspectives. Apple Academic Press, Toronto.

Polson, E.J., Buckman, J., Bowen, D.G., Todd, A.C., Gow, M.M., Cuthbert, S.J., 2002. Biofilms on porous building materials: friend or foe? In 9th International Conference on Durability of Building Materials and Components.

Pozo-Antonio, J.S., Rivas, T., Carrera, F., García, L., 2018. Deterioration processes affecting prehistoric rock art engravings in granite in NW Spain. Earth Surface Processes and Landforms 43, 2435-2448.

584 Rifón Lastra, A., 2000. Algas epilíticas en monumentos de interés históricos de Galicia.
585 PhD thesis, Universidade de A Coruña, Spain.
586
587 Rifón Lastra, A., Noguerol Seoane, A., 2001. Green algae associated with the granite
588 walls of monuments in Galicia (NW Spain). Cryptogamie, Algologie 22 (3), 305-326.
589
590 Rindi, F., Guiry, M.D., 2004. Composition and spatial variability of terrestrial algal
591 assemblages occurring at the bases of urban walls in Europe. Phycologia 43, 225-235.
592
593 RILEM (Reunion Internationale des Laboratoires d'Essais et de Recherche sur les
594 Materiaux et les Constructions). 1980. Commission 25 PEM. Protection et Erosiondes
595 Monuments. Recommandations provisoires. Essais recommandes pour mesurer
596 l'alteration des pierres et evaluer l'efficacite des methodes de traitement [French]. Test
597 No. II. 1: Open porosity and Test II. 2: Bulk and real densities.
598
599 Rivas, T., 1997. Mecanismos de alteración de rocas graníticas utilizadas en la
600 construcción de edificios antiguos de Galicia. PhD thesis, Universidade de Santiago de
601 Compostela, Spain.
602
603 Rivas, T., Prieto, B., Silva, B., 2000. Influence of rift and bedding plane on the physico-
604 mechanical properties of granitic rocks. Implications for the deterioration of granitic
605 monuments. Building and Environment 35, 387-396.
606
607 Rueden, C.T., Schindelin, J., Hiner, M.C., DeZonia, B.E., Walter, A.E., Eliceiri, K.W.,
608 2017. ImageJ2: ImageJ for the Next Generation of Scientific Image Data. BMC
609 Bioinformatics 18, 529.
610
611 Sanmartín, P., Rodríguez, A., Aguiar, U., Medium-term field evaluation of several
612 widely used cleaning-restoration techniques applied to algal biofilm formed on a
613 granite-built historical monument. International Biodeterioration and Biodegradation,
614 this issue.
615
616 Sanmartín, P., Fuentes, E., Montojo, C., Barreiro, P., Paz-Bermudez, G., Prieto, B.,
617 2019. Tertiary bioreceptivity of schists from prehistoric rock art sites in the Côa Valley
618 (Portugal) and Siega Verde (Spain) Archaeological Parks: effects of cleaning
619 treatments. International Biodeterioration and Biodegradation 142, 151-159.
620
621 Silva, B., Sanmartín, P., Prieto, B., 2019. Characterization of the support rock of the
622 petroglyphs of Campo Lameiro (Pontevedra). Cadernos do Laboratorio Xeolóxico de
623 Laxe vol. 41 (In Spanish). ISSN: 0213-4497.
624
625 Socrates, G., 2001. Infrared and Raman Characteristic Group Frequencies: Tables and
626 Charts, 3rd edn. John Wiley & Sons: Baffins Lane, Chichester.
627

628 Steffgen, T., 2019. Experimental studies - Building physics investigations in
629 condensation water on plaster surfaces Pollack Periodica 14(1), 167-175.
630
631 Thornbush, M.J., 2013. Digital Photography Used to Quantify the Greening of North-
632 Facing Walls along Broad Street in Central Oxford, UK. Royaume-Uni.
633 Geomorphologie: Relief, Processus, Environment 2, 111-118.
634
635 Thornbush, M.J., 2014. Orientational Effects on Soiling Measurements at the
636 Sheldonian Theatre in Central Oxford, UK. Journal of Buildings Research, Conscientia
637 Beam, vol. 1(1), 1-27.
638
639 UNE-EN 1936:1999. Natural stone test methods, Determination of real density and
640 apparent density, and of total and open porosity, AENOR (Spanish Association for
641 Standardisation and Certication).
642
643 Vázquez-Nion, D., Silva, B., Prieto, B., 2018. Influence of the properties of granitic
644 rocks on their bioreceptivity to subaerial phototrophic biofilms. Science of the Total
645 Environment 610–611, 44–54.
646
647 Viles, H., Ahmad, H., 2016. Architectural controls on the bioreceptivity of sandstone to
648 green algal colonization. ECBSM2016. European Conference on Biodeterioration of
649 Stone Monuments - Second Edition. Cergy-Pontoise, France. November 17–18, 2016.
650
651 Villa, F., Remelli, W., Forlani, F., Gambino, M., Landini, P., Cappitelli, F., 2012.
652 Effects of chronic sub-lethal oxidative stress on biofilm formation by *Azotobacter*
653 *vinelandii*. Biofouling 28, 823–833.
654
655 Villa, F., Pitts, V., Lauchnor, E., Cappitelli, F., Stewart, P.S., 2015. Development of a
656 Laboratory Model of a Phototroph-Heterotroph Mixed-Species Biofilm at the Stone/Air
657 Interface. Frontiers in Microbiology 6, 1251.
658
659 Vojtková, H., 2017. Algae and their biodegradation effects on building materials in the
660 Ostrava industrial agglomeration IOP Conference Series: Earth and Environmental
661 Science. 92(1), 012073.
662
663 Wurtz, A., 1944. Remarques sur une Pleurococcacée: *Apatococcus vulgaris* Brand.
664 Bulletin de la Société Botanique de France 91 (7/8), 185-190.
665
666 XLSTAT 2019: Data Analysis and Statistical Solution for Microsoft Excel. Addinsof,
667 Paris, France.
668
669 Zhang, G., Gong, C., Gu, J., Katamaya, Y., Gu, J.-D., 2019. Biodeterioration and the
670 mechanisms involved of sandstone monuments of World Cultural Heritage sites in
671 tropical regions. International Biodeterioration and Biodegradation 143, 104723.

672 **Figure legends**
673
674 Figure 1. The four background walls of the processional cloister of the Monastery of
675 San Martiño Pinario. N: north-facing wall, S: south-facing wall, E: east-facing wall, W:
676 west-facing wall.
677
678 Figure 2. Confocal laser scanning imaging of the biofilm collected from the most
679 hydrophobic areas. Colour key: phototrophs, blue (autofluorescence); total
680 chemotrophs, green (Syto9); extracellular glycoconjugates, red (Con A); stone, grey
681 (reflection). Scale bars are 100 μm.
682
683 Figure 3. (A) General appearance of the biofilm, with drops of water suspended after
684 moistening, photographed with a digital camera. (B) Detail of the moistened biofilm,
685 photographed with a digital microscope (Dino-Lite AM3113T). (C) *Apatococcus*
686 *lobatus* cell morphology observed under a light microscope (Nikon Eclipse 50i). Scale
687 bar = 50 μm (B); 5 μm (C).
688
689 Figure 4. Contact angle (degree) and WDPT: water drop penetration time (s).
690 Photographs and microphotographs of samples with (A.1) biofilm with highest water
691 repellency, (A.2) biofilm with lowest water repellency, (B) granite surface after removal
692 of the biofilm, (C) algal cells without the extracellular matrix on a nitrocellulose
693 membrane, (D) nitrocellulose membrane. Water repellency categories according to
694 Leelamanie et al. (2008).
695 Asterisk indicates that measurements were made immediately after placing the drop of
696 water on the surface.
697 3 s and 10 s: Photographs taken 3 and 10 seconds after placing the drop of water on the
698 surface.
699
700 Figure 5. Photographs of fragments of samples from background walls of the
701 processional cloister. A-B) Uncolonized granite surface; C-E) Colonized granite surface
702 with *A. lobatus* algal biofilm; F) Detail of *A. lobatus* sarcinoid aggregrates. Scale bar =
703 150 μm (A, B); 250 μm (C); 100 μm (D, E); 25 μm (F).
704
705
706 Figure S1. Arch in the central courtyard with the pattern outlined by the biofilm growth
707 and sunlight projecting on the background walls of the processional cloister.
708
709 Figure S2. Box plots of the EPS components. A) Polysaccharide content (micrograms
710 per milligrams of the total biomass of the biofilm). Asterisk above the whisker indicates
711 significant difference between means according to the Mann–Whitney U-test (U = 34.0;
712 p-value = 0.009) performed after that Kruskal Wallis test showed significant differences
713 between 1 - 2 and 3 – 4 (H = 6.987; p-value = 0.075). B) Protein content (μg per mg of
714 the total biomass of the biofilm), Kruskal-Wallis test showed no significant difference
715 (H = 3.101; p-value = 0.376).

Figure S3. Correlation between EPS components and the contact angle values. The strength of linear relationship between paired data is indicated by Pearson's correlation coefficient (R) and t test of the regression slope (significant at $p < 0.05$).

Figure S4. ATR-FTIR spectra obtained from the granite samples from uncolonized adjacent areas (N1-N3) and from underneath the biofilm (U1-U3). Y-axis: absorbance (A.U.). X-axis: wavenumber (cm^{-1}).

Video S1. Water repellency of *A. lobatus* subaerial biofilm.


N


S


E


W

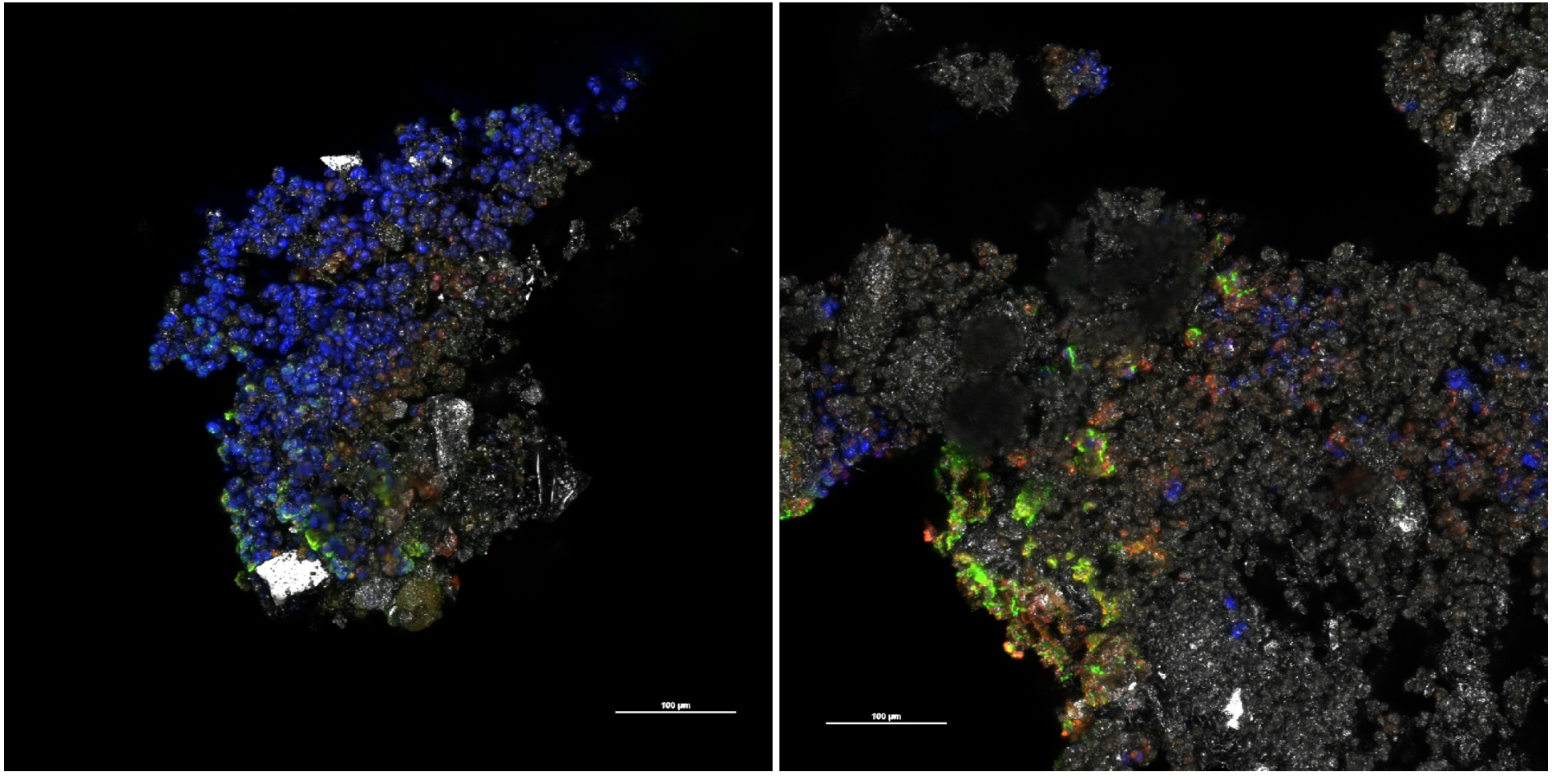
100 µm
100 µm

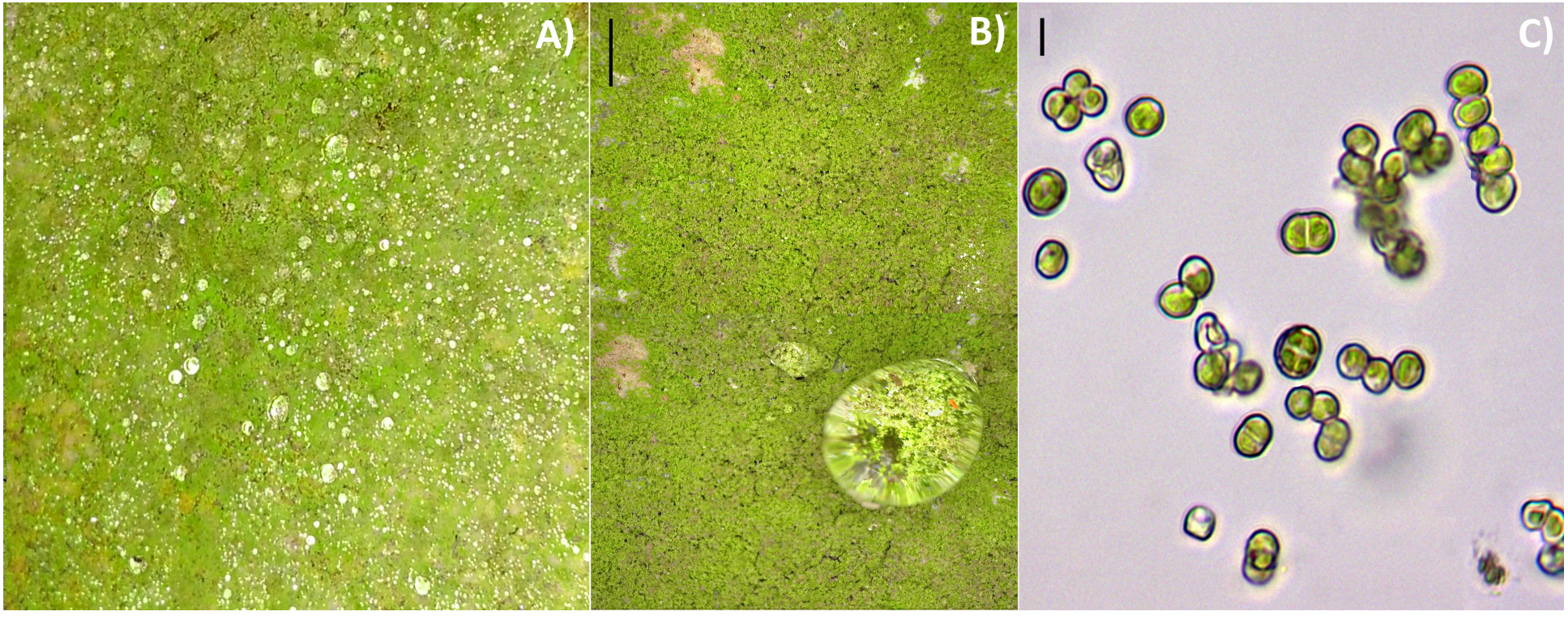
A)
B)
C)

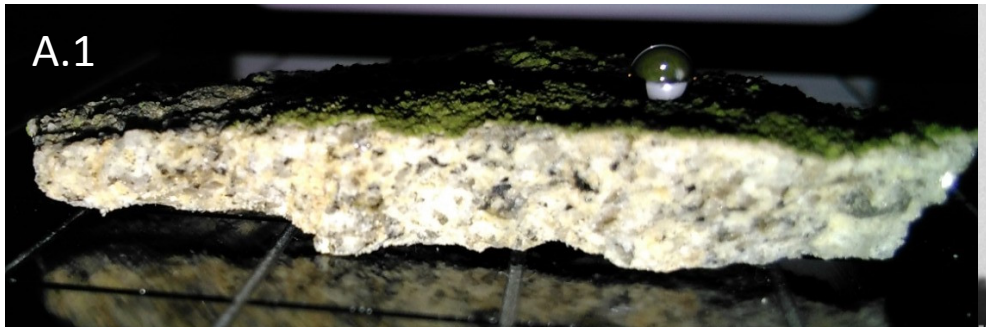

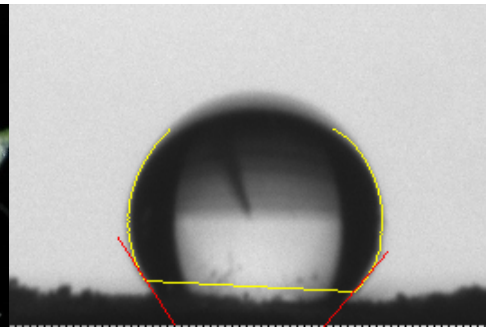

Contact angle (degree):
133.5 ± 3.5

WDPT (s):
≥ 3600, Extremely repellent

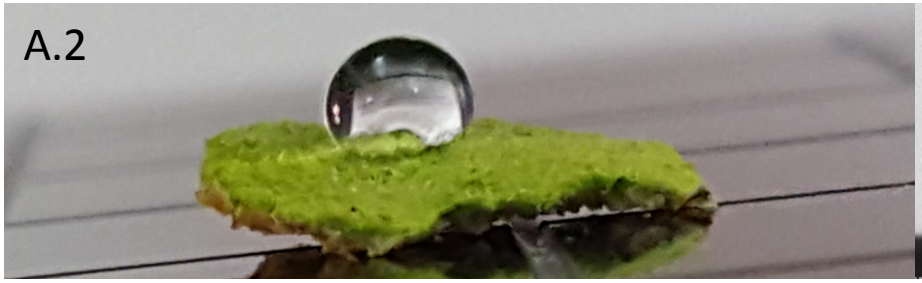

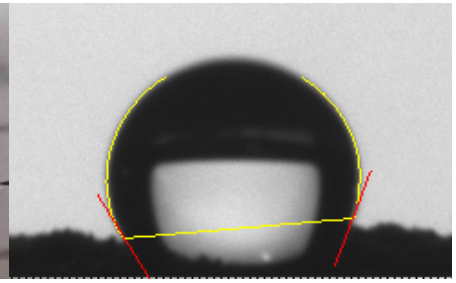

Contact angle (degree):
119.4 ± 4.8

WDPT (s):
≥ 3600, Extremely repellent

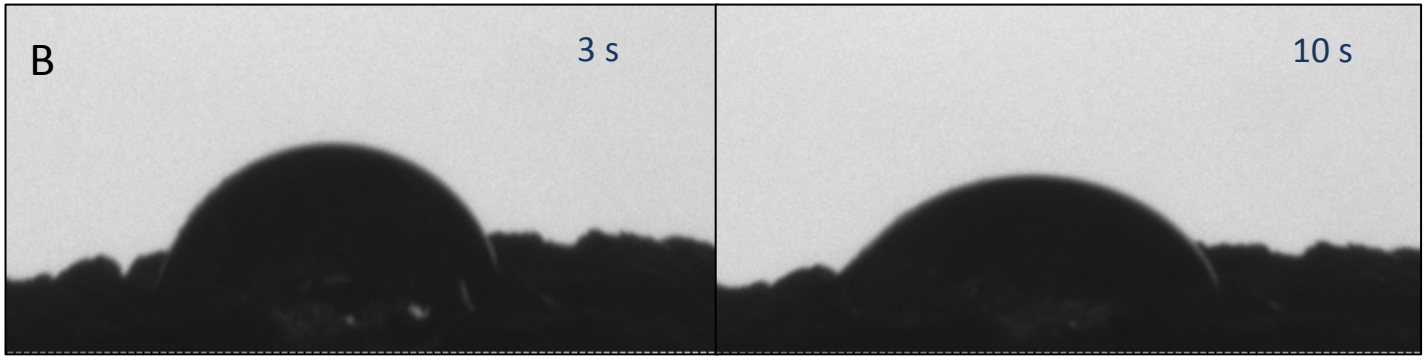

Contact angle (degree)*:
101.9 ± 4.9

WDPT (s):
60-600, Strongly repellent

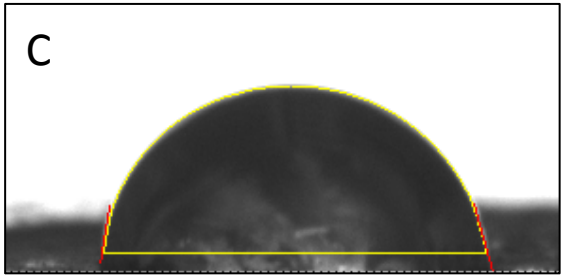

Contact angle (degree)*:
85.6 ± 2.7

WDPT (s):
≤ 1, Non-repellent

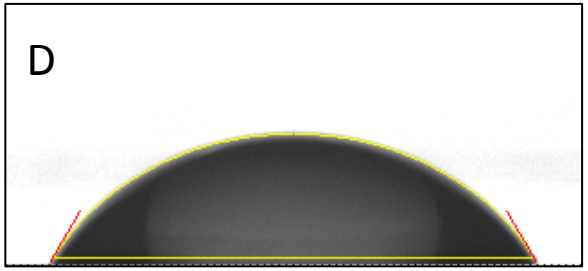

Contact angle (degree)*:
58.7 ± 1.0

WDPT (s):
≤ 1, Non-repellent

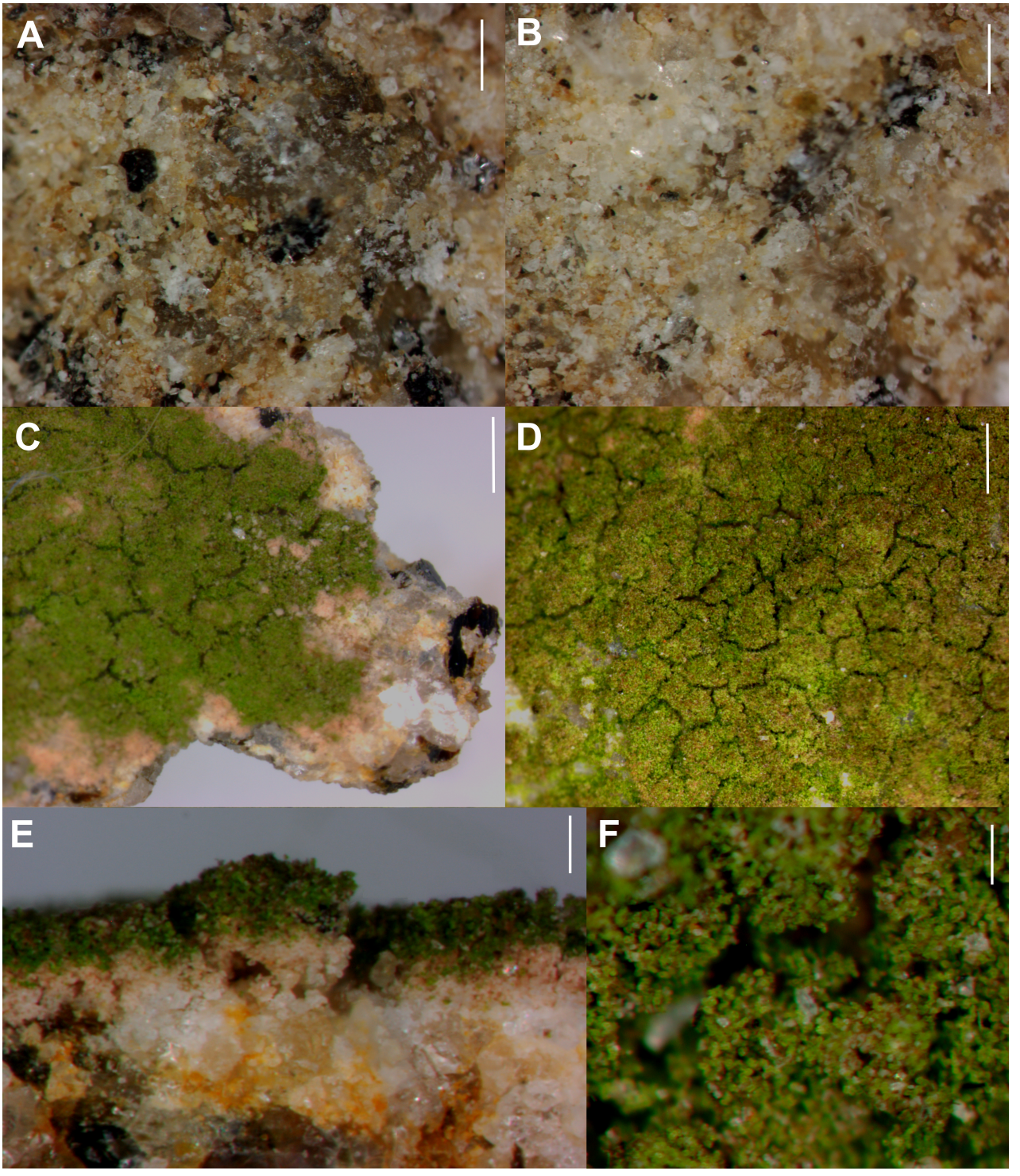
A
B
C
D
E
F


USC

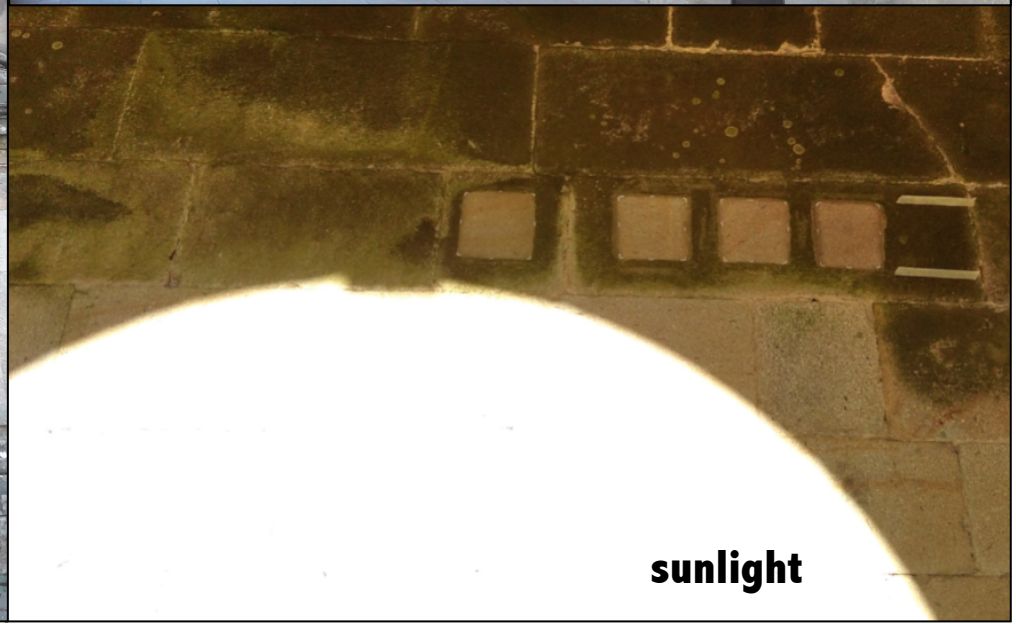
sunlight

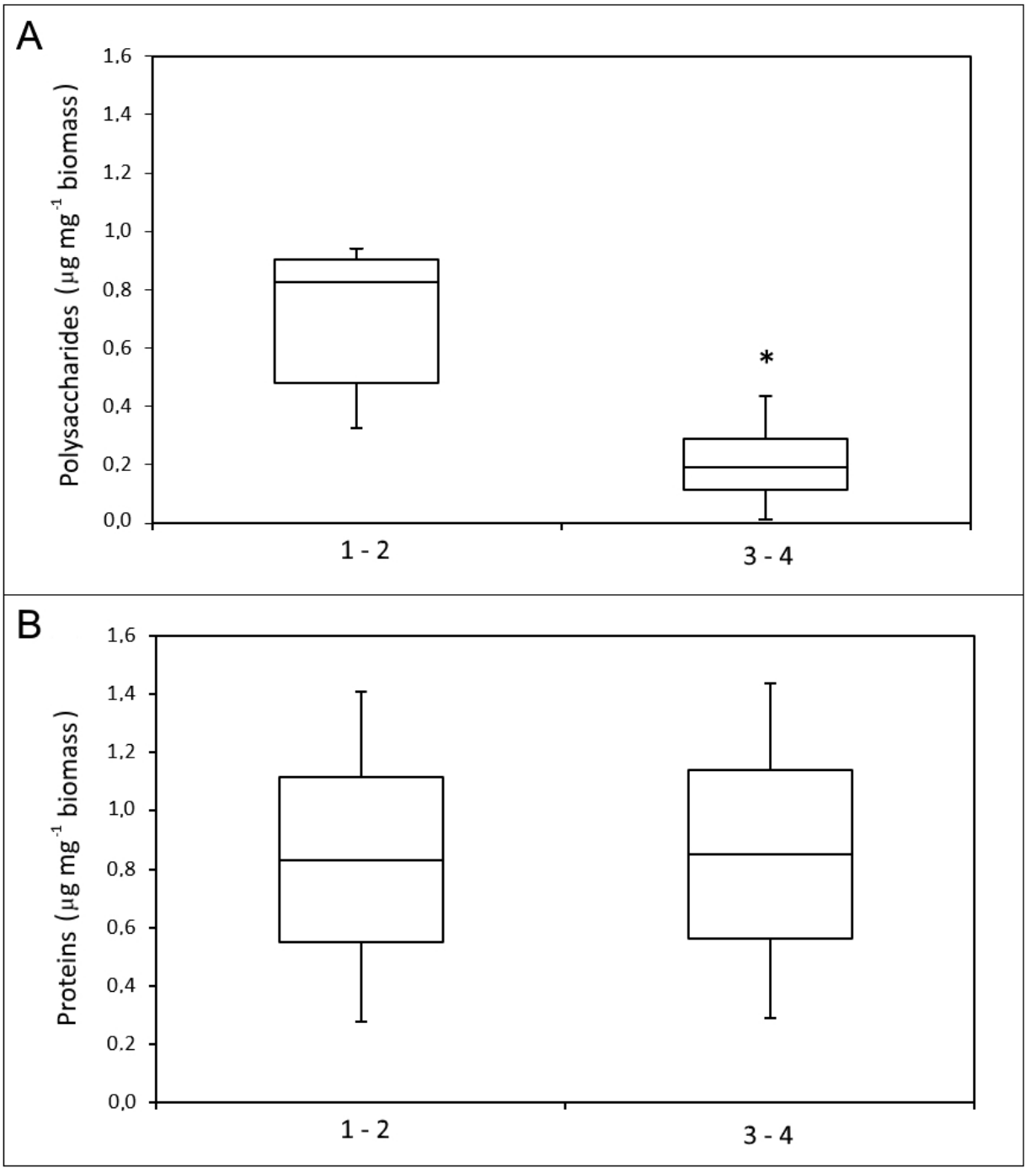
A
Polysaccharides (µg mg-1 biomass)
1,6
1,4
1,2
1,0
0,8
0,6
0,4
0,2
0,0
*
1 - 2
3 - 4
B
Proteins (µg mg-1 biomass)
1,6
1,4
1,2
1,0
0,8
0,6
0,4
0,2
0,0
1 - 2
3 - 4

A

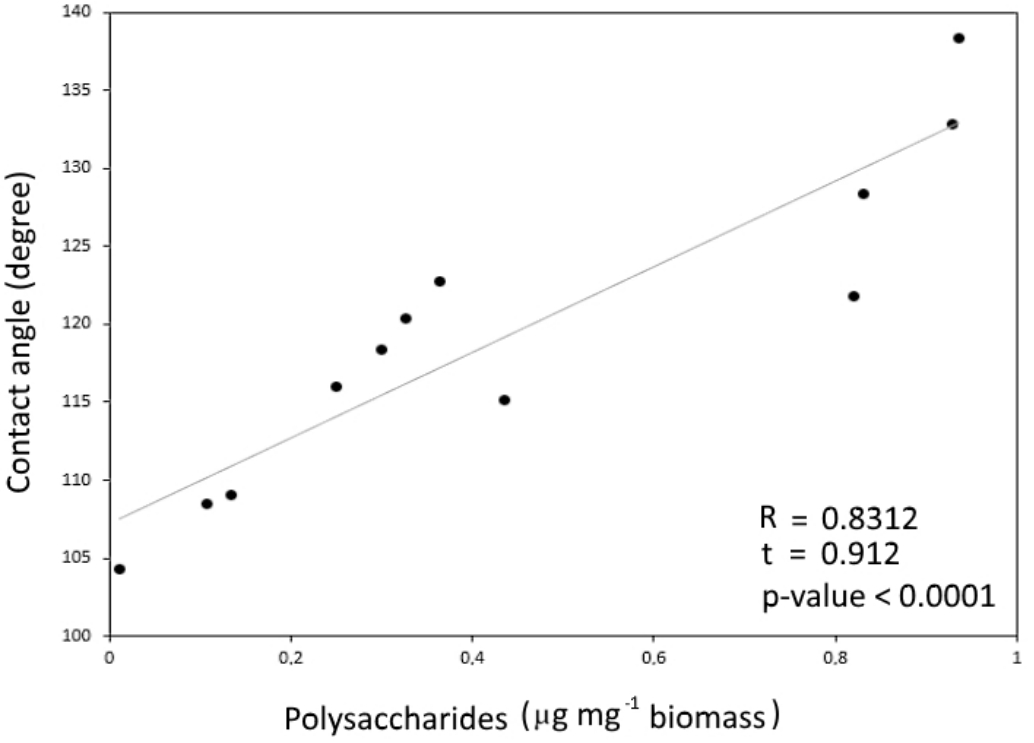
Contact angle (degree)
140
135
130
125
120
115
110
105
100
0
0,2
0,4
0,6
0,8
1
R = 0.8312
t = 0.912
p-value < 0.0001
Polysaccharides (µg mg-1 biomass)

B

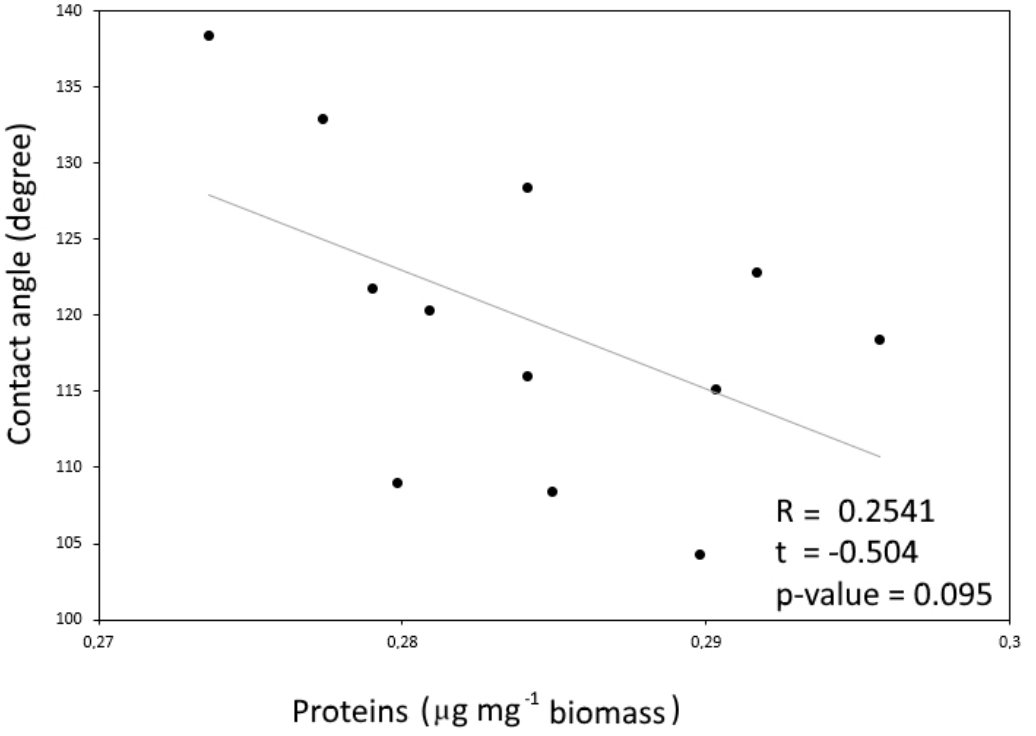
Contact angle (degree)
140
135
130
125
120
115
110
105
100
0,27
0,28
0,29
0,3
R = 0.2541
t = -0.504
p-value = 0.095
Proteins (µg mg-1 biomass)

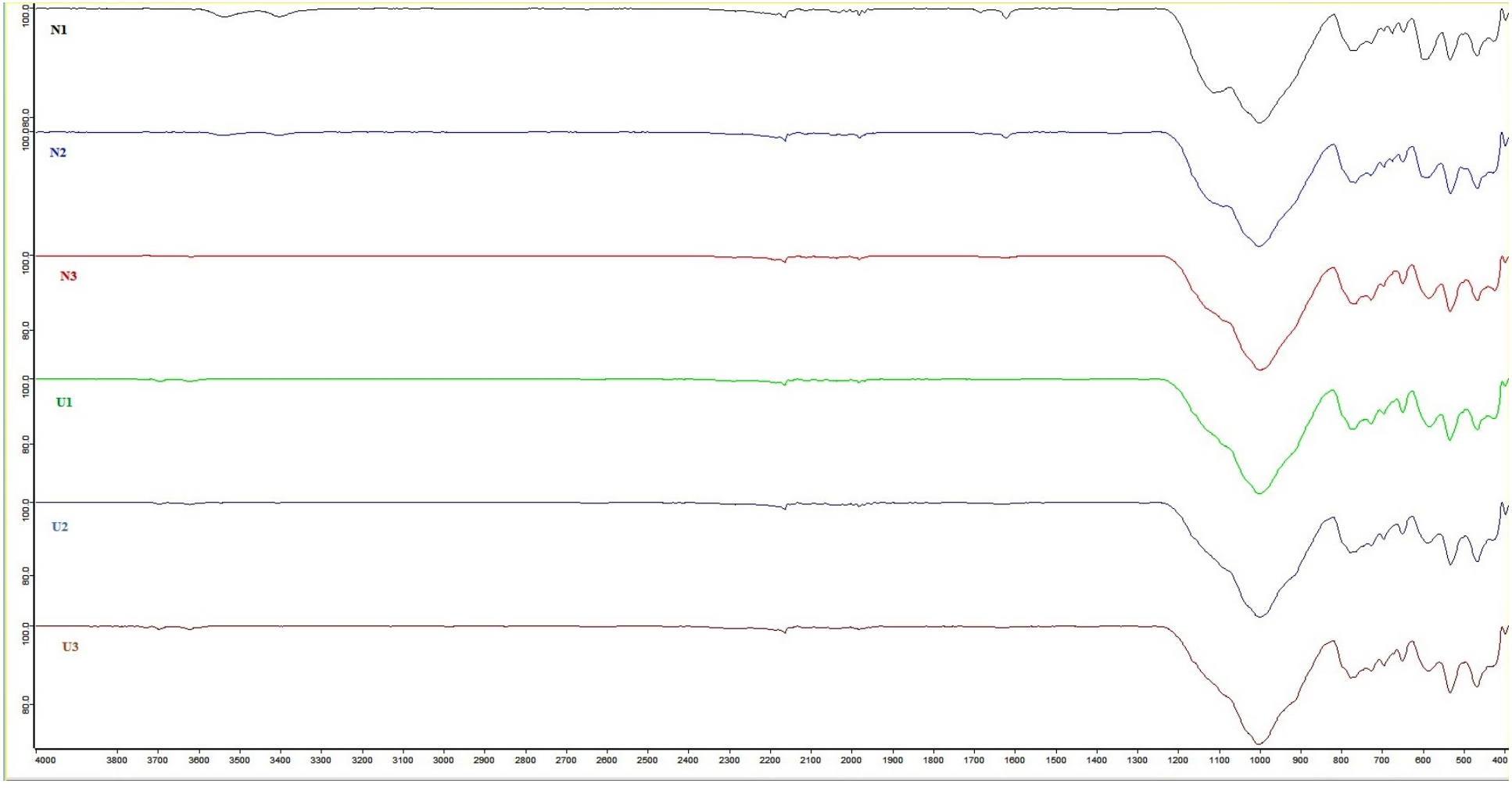
N1
N2
N3
U1
U2
U3
100.0
80.0
4000
3800
3700
3600
3500
3400
3300
3200
3100
3000
2900
2800
2700
2600
2500
2400
2300
2200
2100
2000
1900
1800
1700
1600
1500
1400
1300
1200
1100
1000
900
800
700
600
500
400

Table 1. Composition of the biofilm matrix. Polysaccharide and protein contents (mean ± SD, µg per mg of the total biomass of the biofilm) and percentage (%) of each exopolymeric saccharide matrix. Different letters in the first two columns indicate significant differences (p-value < 0.05) between samples.

Sample	Polysaccharide content (µg mg^{-1} biomass)	Protein content (µg mg^{-1} biomass)	Polysaccharide content (%)	Protein content (%)
1	0.744 ± 0.3328 $_A$	0.280 ± 0.010 $_A$	72.7	27.3
2	0.6659 ± 0.289 $_A$	0.281 ± 0.003 $_A$	70.1	29.9
3	0.185 ± 0.222 $_B$	0.2988 ± 0.003 $_A$	39.1	60.9
4	0.2329 ± 0.085 $_B$	0.2986 ± 0.0108 $_A$	44.5	55.5

Santiago de Compostela, Spain. July 31, 2019

Disclosure of potential conflict of interest

The authors declare that they have no conflicts of interest.

Patricia Sanmartín, on behalf of the authors.

Patricia Sanmartín
Departamento de Edafoloxía e Química Agrícola
Facultade de Farmacia. Pavillón A - Soto. Campus Vida
Universidade de Santiago de Compostela
15782 Santiago de Compostela (A Coruña). SPAIN.
Tel : +34 881814984
https://orcid.org/0000-0002-5733-8833
http://webspersoais.usc.es/persoais/patricia.sanmartin/

Characterization of a biofilm and the pattern outlined by its growth on a granite-built cloister in the Monastery of San Martiño Pinario (Santiago de Compostela, NW Spain)

P. Sanmartín [1*], F. Villa [2], F. Cappitelli [2], S. Balboa [3], R. Carballeira [1,4]

1. Departamento de Edafoloxía e Química Agrícola. Facultade de Farmacia. Universidade de Santiago de Compostela, 15782 - Santiago de Compostela, Spain.
2. Dipartimento di Scienze per gli Alimenti, la Nutrizione e l'Ambiente (DeFENS). Università degli Studi di Milano, Via Celoria 2, 20133 - Milano, Italy.
3. Departamento de Microbioloxía e Parasitoloxía, CIBUS-Facultade de Bioloxía and Instituto de Acuicultura, Universidade de Santiago de Compostela, 15782 - Santiago de Compostela, Spain.
4. Centro de Investigacións Científicas Avanzadas (CICA), Facultade de Ciencias, Universidade da Coruña, A Coruña, Spain.

*Corresponding author: Patricia Sanmartín
Telephone: +34 881814984 Fax: +34 881 815106
E-mail address: patricia.sanmartin@usc.es

Full postal address: Patricia Sanmartín Sánchez
Departamento de Edafoloxía e Química Agrícola
Facultade de Farmacia. Pavillón A - Soto. Campus Vida
Universidade de Santiago de Compostela
15782 Santiago de Compostela, A Coruña. Spain

Abstract

The upper zone of the background walls of the processional cloister of the Monastery of San Martiño Pinario (Santiago de Compostela, Galicia, Spain) is affected by a deep green, highly hydrophobic subaerial biofilm. The pattern that the biofilm follows the walls suggests that particular microclimatic conditions induce changes in the biofilm properties. To test this hypothesis, taxonomic and structural identification of the biofilm was carried out by respectively light microscopy and confocal laser scanning microscopy. In addition, the chemical composition was determined by quantification of extracellular polymeric substances in the extracellular matrix of the biofilm, and hydrophobicity was determined by contact angle and water drop penetration time of biofilm and cells. Furthermore, the bioprotective or biodeteriorative role of the biofilm on the cloister is discussed on the basis of the results of stereoscopic microscope observations, X-ray diffraction and attenuated total reflectance-Fourier transform infrared spectroscopy analysis of granite samples from uncolonized areas and from underneath the biofilm. The findings showed that *Apatococcus lobatus* is the predominant algae in the biofilm. The presence of this alga is favoured by water condensation and it neither damages nor protects the substrate, only causing an aesthetic impact.

Keywords: *Apatococcus lobatus*; biodeterioration; cultural heritage; extracellular matrix (ECM); hydrophobicity; subaerial biofilm (SAB).

1. Introduction

The patterns and drivers of biological colonization on buildings, which is closely related to the bioreceptivity concept (Guillite, 1995), is an interesting and topical field of study. Although bioreceptivity is determined by intrinsic characteristics of the substrate such as roughness and porosity (Guillite, 1995; Miller et al., 2012; Vázquez-Nion et al., 2018; Sanmartín et al., 2019), other factors such as the slope angle, surface geometry and degree of shading (Viles and Ahmad, 2016), presence of synthetic polymers (Cappitelli et al., 2004) and also surface colour (Gambino and Sanmartín et al., 2019) have been found to influence phototrophic colonization.

Green algae (chlorophytes) and cyanobacteria (cyanophytes) colonize stonework whenever moisture, light, temperature and nutrient conditions are favourable. According to Liu et al. (2018), stone porosity, temperature and available water/moisture are the critical factors triggering biological colonization on stone surfaces. The duration of damp periods and cooler temperatures strongly affect phototrophic biofilm formation (Ortega-Calvo et al., 1995; Nugari et al., 2009). Under tropical climate conditions, intense sunlight, together with natural rainwater, also strongly promotes colonization (Zhang et al., 2019). Phototrophic biofilms usually occur on damp patches (caused by rainfall) on walls (Gorbushina, 2007; Charola et al., 2008). In France and Germany, north- and west-facing walls are more affected by precipitation (Barberousse et al., 2007), while in the city of Oxford (UK), south- and west-facing walls are more strongly affected (Thornbush, 2014). Heavy precipitation can also cause microorganisms to be removed from the walls. Indeed, in order to measure urban greening in Oxford, Thornbush (2013) selected the north-facing sides because these are usually most prone to presence of phototrophs.

Light is also an important factor controlling phototrophic growth. The ubiquitous green alga *Trentepohlia* sp. grows in very humid areas. It often occurs on concrete, which is porous and retains much water, in areas with sufficient light, although not direct sunlight (Ariño and Saiz-Jimenez, 1996). In poorly lit areas, cyanobacteria are more competitive than algae, covering zones where lichens, which need dry substrates with abundant light, are almost totally absent (Ariño and Saiz-Jimenez, 1996). The phototrophic community may be mainly composed of eukaryotic algae or cyanobacteria, depending on the light exposure. This is the case of the Khmer temples in Angkor (Cambodia), where the initial pioneer community is primarily composed of a reddish biofilm of a green alga that occurs in dry, shady conditions, whereas cyanobacteria prevail in dry, sunny conditions (Caneva et al., 2015).

A number of papers report that phototrophic microorganisms can cause damage to different types of stone and that deterioration is primarily due to the physical features of the stone surface, microclimate and environmental conditions and secondarily to the lithotype (as reviewed in Macedo et al., 2009). By contrast, some papers claim that lichens can protect stone from damage as in the 'Casa Lis', in Salamanca, Spain, which

is built from highly porous Villamayor sandstone (Grondona et al., 1997). Other sessile phototrophic microorganisms can act as protective agents for stone materials (Cutler et al., 2013; Pinna, 2017).

The monastery of San Martiño Pinario (UTM 29T X 537220, Y 4747793; Datum ETRS89) is one of the most emblematic buildings in Galician culture and the second most important historical building (after the Cathedral) in the city of Santiago de Compostela (UNESCO World Heritage City since 1985, capital of Galicia, north-western Spain). The processional cloister, built between 1633 and 1747 (for more information, see Sanmartín et al., this issue), has a deep green, highly hydrophobic subaerial biofilm in the upper zone of the background walls in areas protected from rainfall. This biofilm, reported to be present at least for 50 years, was characterized in detail in the present study, and the taxonomic identification, architecture and extracellular matrix are reported. Its bioprotective or biodeteriorative role was also considered by comparing results obtained by stereoscopic microscope, X-ray diffraction and Fourier Transform infrared analysis of granite samples from uncolonized areas and from underneath the biofilm.

2. Materials and methods

2.1. Colonization pattern and masonry description

The biofilm occurs at a height of about 3 meters, sheltered from rain and direct sunlight and mainly concentrated on north- and west-facing walls (Figure 1). The biofilm is highly water repellent (hydrophobic) (Video 1, supplementary material). The biofilm is present on the surface of the granite ashlars and absent from the joint mortar. The background walls of the cloister are formed by granite masonry, a migmatic granitoid with preferred orientation of biotite and hypidiomorphic granular texture (Rivas et al., 2000). Its open porosity (following RILEM 1980), closely related to the water saturation capacity, is 4.6% ~~(v·v^{-1})~~ (Rivas et al., 2000), which is high in comparison with the open porosity values of 0.1 to ~~1~~2% ~~(v·v^{-1})~~ usually observed in sound granitic rocks (UNE-EN 1936:1999; Silva et al., 2019). The porosity of granite increases with the inter- and intra-granular fissures and a well-connected network of fissures, as well as the presence of clay minerals such as chlorite, kaolinite and vermiculite. According to Rivas (1997), the ashlar rock in the processional cloister of the Monastery of San Martiño Pinario displays a high degree of fissuring, especially in the —upper three centimetresc~~m~~, while its modal composition comprises quartz (49%), plagioclase (12%), alkaline feldspar (microcline-9%), muscovite (16%) and biotite (partly chloritized-12%), as main minerals, and kaolinite and vermiculite in trace amounts (<3%).

The joint mortar was analysed in the present study by X-ray diffraction (XRD), in a PW1710 Philips diffractometer equipped with a PW1820/00 goniometer and an Enraf Nonius FR590 generator operating at 40 kV and 30 mA. The X-rays were obtained with CuKα-radiation (λ = 1.5406 Å), and the XRD diffractogram patterns were acquired in

the angular range of $2<2\theta<65$ with a step size of 0.02° and a measuring time of 2 s per step. Identification of the minerals was made by comparison with the ICSD and COD databases.

The pH of granite and joint mortar was measured with pH-Universal indicator strips (MERK) after contact for 60 ± 5 seconds, according to the American Standard ASTM F710.

2.2. Biofilm architecture

Biofilm samples were collected using the non-invasive method with adhesive tape strips. Strips were gently applied to the stone surface and then placed on sterile glass microscope slides and transported in a box to the laboratory. The adhesive tape strips were then immediately analysed by confocal laser scanning microscopy (CLSM).

Confocal images were collected using a Nikon A1 laser scanning confocal microscope and a 20x/0.75NA (WD 1 mm) Plan Apo λ objective. Fluorescence was excited and collected using different combinations of the following laser lines and emission parameters: i) autofluorescence from photosynthetic pigments was viewed in the blue channel using the 633 nm line of an Ar/HeNe laser in the emission range of 650 to 750 nm; ii) EPS were labelled with the lectin Concanavalin-A- Texas red (Molecular Probes, Inc., Eugene, OR, USA) (final concentration, 0.8 mmol~~mM~~) and observed in the red channel (excitation at 561 nm line, and emission at 590 to 630 nm); iii) chemotrophs were visualized in green (excitation at 488 nm line, and emission at 500 to 550 nm) after staining with Syto9 (final concentration, 50 µmol~~M~~).

CLSM was used in reflectance mode with the 488 nm argon line for relief imaging of specimens. Captured images were analysed with NIS-Elements software (Nikon) for 3D reconstruction of biofilms.

2.3. Taxonomic identification

The subaerial biofilm was first examined on site with a Dino-Lite AM3113T digital handheld microscope with DinoXcope Imaging Software. Subsequently, ten micro-samples of biofilm were removed from several areas of the background walls of the processional cloister with the aid of scalpel and placed sterile plastic tubes, for identification by light microscopy. Five areas of 20 cm^{2}~~3~~ were scraped from the walls for biomass determination. The micro-samples were examined under a stereoscopic microscope (Nikon Eclipse E600, Tokyo, Japan) equipped with an E-Plan x40 objective (N.A. 0.65) and differential interference contrast (Nomarski) optics. Light microscopy photographs were taken with an AxioCam ICc5 Zeiss digital camera. Taxonomic determinations were based on the morphometry and reproduction of the species in culture, following the taxonomic criteria of Ettl and Gäertner (1995), Rifón-Lastra (2000), Rifón-Lastra and Noguerol-Seoane (2001) and Rindi and Guiry (2004).

2.4. Wetting characterization by contact angle analysis

A Drop Shape Analyzer DSA 100 (Krüss GmbH, Hamburg, Germany) was used for water repellency measurements: a droplet of distilled water (10 µL) was deposited onto the target surface and the water-surface contact angle was immediately measured. No fewer than 5 measurements were made on different zones of the target surface at 25 °C. The contact angle was measured on digital microphotographs with Image J2 software (Rueden et al. 2017). The water drop penetration time (WDPT) test was conducted according to Leelamanie et al. (2008).

During the first observations (section 2.3.), a simple on-site test with a wash bottle indicated that some parts of the biofilm were more hydrophobic than others. For this reason and for global characterization of the biofilm, measurements were made in biofilm samples with greater and lower degrees of water repellency. In addition, and for comparative purposes, measurements were made on uncolonized granite, granite underneath the biofilm and algal cells, after extracting the extracellular matrix.

2.5. Extracellular polymeric substances (EPS)

Four areas (each 18 cm^2) of the colonized upper zone of the background walls of the cloister were scraped to remove the biofilm. The cells of the exopolymeric matrix (EPS) were then separated and the main components were identified: carbohydrates (polysaccharides) and proteins.

As in section 2.4., EPS analysis was performed in samples taken from the most hydrophobic areas (samples 1 and 2) and from the less hydrophobic areas (samples 3 and 4).

Approximately 1.5 g of biofilm sample was obtained in each area and split into three subsamples. The EPS extraction was performed following Villa et al. (2015), with a slight modification. Briefly, 0.04 g of each subsample was resuspended in 2 mL~~l~~ 2% ethylenediaminetetraacetic acid by vortexing and sonication in a bath (45 kHz) for 10 min. Samples were vortexed again and shaken at 300 rpm for 3 h at 4ºC. To separate the cell debris from the supernatant containing the EPS, the samples were filtered through 0.22 µm nitrocellulose membranes (Millipore). The EPS was then precipitated overnight in two volumes of chilled ethanol at -20ºC, centrifuged at 13000 rpm for 30 min at 4ºC and washed twice with 95% ethanol. Samples were then air-dried and resuspended in 380 µL~~l~~ of M9 mineral medium. Each subsample was then diluted in distilled water, and the carbohydrate content of the EPS was measured by the phenol-sulfuric method, with glucose as standard. The amount of carbohydrate or polysaccharide content was expressed as the mean ratio relative to the dry biomass, following Villa et al. (2012). The protein content was measured following the Bradford assay (Bradford, 1976) in microtitre plates.

2.6. Analysis of the impact of biofilm on the granite

In addition to the obvious aesthetic biodeterioration, any possible physical and chemical alteration of the granite building material caused by the biofilm was determined by analysis in a stereoscopic microscope (Nikon Model SMZ1500) equipped with a Digital Camera (Nikon DXM 1200) and a digital image capture software (Nikon ACT-1). Fragments of samples with subaerial biofilm were examined, focusing attention on the appearance of the granite under the biofilm. Fragments without subaerial biofilm were also examined for comparative purposes.

Furthermore, three fragments of approx. 2.5 cm x 1.8 cm x 0.2 cm^3 of each of the colonized and uncolonized areas were taken for comparison of the changes triggered by the biofilm in the mineralogical composition and compositional features of granite building material. In the three colonized samples, the biofilm was carefully removed from the stone surface with the aid of a soft brush, and granite samples were obtained from underneath the biofilm (U1-U3) for analysis. The samples were compared with three reference granite samples from adjacent uncolonized areas (N1-N3). The six samples were crushed separately into small particles and ground to a very fine powder (<50 μm the diameter of particle). Each sample was then divided into two equal parts: one for X-ray diffraction study of mineralogical composition and another for attenuated total reflectance-Fourier transform infrared spectroscopy analysis for identification of the components.

For X-ray diffraction (XRD), the same device and conditions described in Section 2.1. were used. The granite samples were turned over to obtain profiles optimal peak for analysis, as well as minimize the effect of preferential orientation.

Attenuated total reflectance-Fourier transform infrared spectroscopy (ATR-FTIR) was carried out in a Varian 670-IR spectrometer (Varian Inc., Santa Clara, CA) equipped with an ATR device with a single-reflection diamond crystal (Pike GladiATR, Madison, WI). The spectra were obtained with an angle of incidence for the infrared beam through the diamond crystal of 45°, in the spectral range of the medium (4000 cm^{-1} to 400 cm^{-1}) and a resolution of 4 cm^{-1}.

2.7. Statistical analysis

The quantities of both EPS components (polysaccharides and proteins) were statistically compared using a Kruskal-Wallis test with Conover-Iman multiple pairwise comparisons at a significance level of 95 % ($\alpha = 0.05$) and Bonferroni correction. Pearson correlation coefficients (R) were calculated for both EPS components and the measured contact angles, and t-test, with a significance level of 95 % ($\alpha = 0.05$). All statistical analyses were performed using XLSTAT 2019 software.

3. Results and discussion

3.1. Characterization of the biofilm and the pattern outlined

The presence of biofilm is visually homogeneous over the surface of the granite ashlars surface (pH 6 to 7). By contrast, the joint mortar is not colonized. It is a lime mortar of pH 8 to 9, with calcite ($CaCO_3$, 23%) and gypsum ($CaSO_4$ $2H_2O$, 3%) as dominant phase, and granite sand with a mineral composition very similar to the ashlars, indicating that crushed quarry material was probably reused as aggregate for the mortar.

Representative images of the biofilm obtained from the granite surface are shown in Figure 2. The images correspond to the Maximum Intensity Projection (MIP) 3D reconstructions obtained from confocal images series with the dedicated NIS-Elements software. The fluorescent signals in Figure 2 detected cells in the biofilms. A patchy distribution of small cell aggregates can be seen to follow the topography of the surfaces.

Overall, the predominance of phototrophic communities (blue signal) was characterised by coccoid structures assembled in clusters, while the Syto9 stain did not reveal an extensive chemotrophic microbial community. However, these communities were highly developed in zones with weak or absent photosynthetic pigment fluorescence. The red signal, derived from the lectin-binding dye Con A, revealed the presence of extracellular glycoconjugates (i.e. polysaccharides, including those covalently linked to proteins and/or lipids) covering the granite surfaces and partly overlapping the blue signal of phototrophs. Overall, the microscopic studies revealed the following: i) the granite substrate is colonized by a monolayer of cells growing in small clusters that follow rock fissures and cracks; ii) phototrophs comprised the largest proportion of the biofilm community in all specimens analyzed; and iii) microbial cells occurred in densely packed ~~EPS-glycoconjugates~~ aggregates surrounded by the EPS matrix~~mineral particles~~.

Taxonomic identification of the biofilm showed that *Apatococcus lobatus* (Chodat) J.B.Petersen (Chlorophyta) was the predominant species, with some of the algae appearing partially lichenized. *A. lobatus* cells are 2.8 - 4.7 µm wide and 5.3 - 18.6 µm long, macroscopically ~~Macroscopically, the cells (2.8 - 4.7 x 5.3 - 18.6 µm)~~ form sarcinoid aggregates with a bright green powdery consistency and up to 100 µm thick (Figure 3). The dry weight per unit area of the biofilm covering the walls was 0.32 ± 0.07 ~~(0.27 - 0.35)~~ g cm^{-2}, and the moisture content of the fresh biofilm was 65 %.

Apatococcus lobatus is a widely documented, cosmopolitan species in subaerial environments and niches, including anthropogenic constructions (Ettl and Gärtner, 1995; Rifón-Lastra, 2000; Rifón-Lastra and Noguerol-Seoane, 2001; Barberousse et al., 2006). It is a species of green algae with mixotrophic metabolism with generally low

growth rates but which increase greatly with organic inputs (Gustavs et al., 2016). This may be an important adaptive advantage in the colonization of acid subaerial habitats (such as granite walls) where bacterial activity is generally lower. This species is one of the most abundant algae in temperate Europe, forming robust biofilms on tree bark and building surfaces (Gustavs et al., 2011). *A. lobatus* has previously been observed colonizing granite outcrops in the Ukraine valleys (Mikhailyuk, 2013).

The presence of *A. lobatus* in subaerial environments protected from rainfall is probably related to its high resistance to desiccation, e.g. due to thickening of the cell wall, which waterproofs the cells and prevents dehydration (Wurtz, 1944), as well as explaining the strong hydrophobic character of the biofilm observed during the study (Figure 3 and Video 1, supplementary material). Similarly, biofilms collected across an altitude range from sea level to around 900 m, along the coast of Lazio (Italy) to 60 -km inland, showed a dominant presence of the filamentous terrestrial green alga *Trentepohlia umbrina* (Kützing) Bornet (Bartoli et al., 2019). Thise algae was found to prefer areas of low relative humidity (RH) on exposed north-facing vertical surfaces. This dominance was explained by the higher nocturnal condensation typical of coastal areas.

Galicia has an oceanic climate with high atmospheric humidity caused by high rainfall and mild temperatures throughout the year (Martínez-Cortizas and Pérez-Alberti, 1999). According to data for the last ten years (2009-2019), the relative humidity (RH) in Santiago de Compostela is between 77 and 85% (www.meteogalicia.gal). A previous study (Bertsch, 1966) investigated the effect of desiccation of *A. lobatus* induced by decreasing air humidity. Although carbon assimilation was reported to be highest at or above 97–98% RH, half of the maximum carbon dioxide-uptake still took place at 90% RH, with the lowest level of carbon assimilation occurring at 68% RH (Bertsch, 1966). These data clearly showed that moisture favoured carbon dioxide uptake by *A. lobatus*, while water had an unfavourable effect, and also showed that average humidity in Santiago de Compostela is not sufficient for the optimal growth of the green alga.

Microclimatic effects affect the pattern outlined by the biofilm growth. First, north- and west-facing walls are clearly more prone to algal colonization growth, which is explained by the fact that algae are transported by wind as spores (Barberousse et al., 2007) as well as by wind-driven precipitation and by the fact that in Galicia the prevailing wind direction is west or north-west (www.meteogalicia.gal; www.meteoblue.com). Second, the biofilm only appears in the areas of the wall shaded from direct sunlight, and the undulating pattern of colonization is explained by the sunlight passing through the central arches of the courtyard (Figure S1). As Barberousse et al. (2007) explain, a gradient of temperature on a facade, with one area cooler than another warmed by the sun, may result in condensation of atmospheric humidity in the first area, favouring algal growth in the cool area. In recent years, various different masonry surfaces have been observed to be covered with algae. In the German town of Rostock, most buildings were constructed in the 1970s using concrete and were renovated in 1993 by adding insulation and artificial resin plaster to the surface. Shortly

afterwards, these coatings became almost totally covered by green microalgae, mainly on the north and west sides, especially in areas not exposed to full solar radiation (Häubner et al., 2006). In a recent paper by Steffgen (2019), the phototrophic growth was related to improved thermal insulation of buildings and the accumulation of condensation was considered of decisive importance.

3.2. Biofilm hydrophobicity

According to the categories of water repellency assigned by Leelamanie et al. (2008), both biofilm samples, seemingly more and less hydrophobic, were found to be extremely repellent to the water, with the time taken for the complete penetration of the water drop of more than an hour and water contact angles of 133.5º ± 3.5º and 119.4º ± 4.8º, respectively (Figure 4). The contact angle could not be measured on uncolonized granite as the drop was absorbed immediately upon falling. The water drop penetration time (WDPT) was less than 0.2 s, corresponding to instantaneous penetration and non-repellent character. The hydrophobicity of the rock where the biofilm was formed was still notable after biofilm removal (contact angle of 101.9º □ 4.9º), although the WDPT value was greatly reduced, by up to 60-600 s, considered strongly repellent (Figure 4). The contact angle of the samples after extraction of the EPS was drastically reduced, to 85.6º ± 2.7º, and the WDPT values of the cells was as low as one second, indicating that they were not water repellent. These values were very similar to those of the nitrocellulose membrane where the cells were deposited: 58.7º ± 1.0º and the same category in the WDPT (Figure 4).

The polysaccharide and protein contents of the biofilm matrix are shown in Table 1. The polysaccharide content of the four samples varied greatly depending on the sampling area, with significant differences in 1 and 2, relative to 3 and 4 (Box plots of the EPS components are presented as supplementary information, Figure S2). In the seemingly most hydrophobic samples (1 and 2), the average polysaccharide content was 0.74 mg/mg $_{dry\ biomass}$ and 0.66 mg/mg $_{dry\ biomass}$ respectively, while the less water-repellent samples (3 and 4) had a carbohydrate content of 0.18 mg/mg $_{dry\ biomass}$ and 0.23 mg/mg $_{dry\ biomass}$, i.e. approximately 3 times lower than their counterparts. ~~In the seemingly most hydrophobic samples (1 and 2), the average polysaccharide content was 0.744 and 0.659 µg/mg$_{drybiomass}$ respectively, while the less water-repellent 3 and 4, had a carbohydrate content approximately 3 times lower than their counterparts, 0.185 and 0.229 µg/mg$_{drybiomass}$.~~ On the contrary, the protein content of the four samples did not differ, with average values of 0.28~~0~~, 0.28~~1~~, 0.29~~88~~ and 0.29~~86~~ µg/mg $_{dry\ biomass}$. Thus, almost three quarters of the EPS were polysaccharides in samples 1 and 2, while in samples 3 and 4, polysaccharides only made up approximately 40-45% of the total EPS (Table 1). Furthermore, the contact angle values and polysaccharides content were highly correlated (R = 0.8312, t = 0.912, p-value < 0.0001), while the correlation with proteins was low (R = 0.2541, ~~(~~t = -0.504, p-value = 0.095). The correlations between EPS components and the contact angle values are presented as supplementary information, Figure S3).

Biofilms can protect masonry materials, also depending on the hydrophilic or hydrophobic features of their matrices. The hydrophilic character of extracellular polymeric substances (EPS) is linked to functional groups of hydrophilic nature such as hydroxyl and carboxyl, as well as phosphate, amine and sulphate, while the hydrophobic character is associated with non-polar regions, such as aromatic and aliphatic regions in proteins and hydrophobic regions in O-methyl/acetyl polysaccharides (Moran, 2009). Extracellular polysaccharides are critical in desiccation tolerance of both cyanobacteria and green algae (Knowles and Castenholz, 2008). Thus, increasing the amount of exopolysaccharides may be a compensatory measure to enhance the efficiency of photosynthesis.

3.3. Role of biofilm on granite conservation

Stereoscopic observations (Figure 5) were consistent with the previous CLSM observations described in section 3.1. Biofilm seems to cover the granite surface by forming aggregates, sometimes surrounding the mineral grains. These grains remained unattached on the surface, and they were observed in the images of the uncolonized granite, with a very sandy surface and visible oxidation of Fe in biotites.

X-ray diffraction (XRD) analysis showed that, relative to the uncolonized granite, the biofilm did not cause any mineralogical changes (Table S1). The mineral composition was very similar in the six samples and semiquantitative measurements coincided with those reported by Rivas (1997). The presence of gypsum in samples N1 and N2 was the only remarkable feature in the XRD analysis (Table S1). Given that gypsum is present in the joint mortar (section 3.1), the most likely hypothesis is that it originates from the mortar and moved to the ashlar.

Analysis of the samples by ATR-FTIR spectroscopy confirmed the lack of mineralogical transformation of the granite (Figure S4). The same bands were seen in all the samples and are representative of the minerals that form granitic rocks, such as the abundant characteristic bands of silicates corresponding to Si-O (quartz), Si-O-Si (quartz), and Si-O-Al (feldspar) in the range 400 – 1100 cm^{-1} (Socrates, 2001; Pozo-Antonio et al., 2018). Only three slightly different signals appeared in the infrared spectra, and none were related to alteration of the granite underneath the biofilm:
(1) The peak with a shoulder at around 1030–1100cm^{-1}, characteristic of silicates and that corresponds to asymmetrical stretching vibration of Si–O (Socrates, 2001; Pozo-Antonio et al., 2018), was present in all the samples. The shoulder, however, was further accentuated in the two samples taken from uncolonized areas N1 and N2, probably by the sum with the peak assigned to gypsum at 1120 cm^{-1} (Socrates, 2001), the only mineral present in these two samples, Table S1). The shoulder disappeared in the samples from under the biofilm (U1-U3) probably by the overlap of the peak with the band at 1040 cm^{-1} corresponding to polysaccharides (Houari et al., 2013) remaining after removal of the biofilm by brushing (section 2.6). The latter is also consistent with the results obtained in the contact angle study (section 3.2).

(2) The weak band at 1630 cm^{-1} that appeared in the uncolonized samples N1 and N2 and that did not appear in the other samples, may be attributed to an organic matter deposit (Madejová and Komadel, 2001), rather than to kaolinite, also associated with this peak but not observed in the X-ray diffraction analysis of either samples (Table S1). (3) The vibrational band assigned to gypsum at 674 cm^{-1} (Socrates, 2001) only appeared in samples N1 and N2 containing the mineral (Table S1).

Green algae colonizing stone surfaces may represent a major problem for the conservation of heritage monuments, and in the last decade evaluation of whether the algal biofilm is causing damage, is neutral or protects the stone substrate has become mandatory (Vojtková, 2017; Pinna, 2017). Several control methods are now available (Pfendler et al., 2018) and can be applied when biodeterioration is demonstrated.

Salt crystal formation, a major cause of stone deterioration, is favoured by water movement in the pores. A hydrophobic layer on the external surface of the wall, which alters the original wettability of that building material, can lead to humidity that inhibits salt crystal formation (Polson et al., 2002). Indeed, it may act as a natural waterproofing agent on the building, possibly preventing the entry of water. Other types of damage that are potentially prevented or reduced include freeze-thaw damage, salt shattering and mineral dissolution. On the other hand, if the water comes from the walls (e.g. by capillary forces or excess condensation from within the building), it is equally possible that this water could be retained behind the biofilm and cause damage. In the Monastery of San Martiño Pinario, these two situations are apparently well balanced and the biofilm has caused neither deterioration nor protection for at least 50 years.

4. Conclusions

The highly hydrophobic ~~biological colonization~~subaerial biofilm in the processional cloister of the Monastery of San Martiño Pinario is mainly formed by *Apatococcus lobatus* (Chodat) J.B.Petersen (Chlorophyta). The study findings showed that the biological growth, promoted by condensation, does not damage or protect the substrate. Indeed, the *A. lobatus* biofilm only has an aesthetic impact on the Monastery walls. On the basis of these results and in view of the future maintenance and conservation of the Monastery building, we recommend that the existing biofilm should not be removed, because it is an interesting case study of a subaerial biofilm and can also be considered part of the cultural heritage in this building. Furthermore, this recommendation is consistent with the 'minimal intervention' concept, i.e. that intervention during heritage conservation activities should be kept to an absolute minimum.

Acknowledgements

This work was financially supported by Xunta de Galicia (grants POS-B/2016/030 and ED431C 2018/32). We thank Carlos Álvarez Varela, dean of the Monastery of San Martiño Pinario, and Eva Varela Rodríguez, secretary of the Seminario Mayor, for

permission to conduct research in the Monastery and for their valuable assistance. The authors also thank Prof. Carmen Álvarez-Lorenzo (Universidade de Santiago de Compostela, Spain) for assistance with contact angle measurements.

References

Ariño, X., Saiz-Jimenez, C., 1996. Colonization and deterioration processes in Roman mortars by cyanobacteria, algae and lichens. Aerobiologia 12(1), 9–18.

ASTM International, 2008. F710-08 Standard Practice for Preparing Concrete Floors to Receive Resilient Flooring.

Barberousse, H., Tell, G., Yéprémian, C., Couté, A., 2006. Diversity of algae and cyanobacteria growing on buildings facades in France. Algological Studies 120, 81-105.

Barberousse, H., Ruot, B., Yéprémian, C., Boulon, G., 2007. An assessment of façade coatings against colonisation by aerial algae and cyanobacteria. Building and Environment 42(7), 2555–2561.

Bartoli, F., Ellwood, N.T.W., Bruno, L., Ceschin, S., Rugnini, L., Caneva, G., 2019. Ecological and taxonomic characterisation of *Trentepohlia umbrina* (Kützing) Bornet growing on stone surfaces in Lazio (Italy). Annals of Microbiology, in press.

Bertsch, A., 1966. CO_2-Exchange and water relations in the aerophillic green-alga *Apatococcus lobatus*. Planta 70(1), 46-72.

Bradford, M.M., 1976. A rapid and sensitive method for the quantitation of microgram quantities of protein utilizing the principle of protein-dye binding. Analytical Biochemistry 72, 248–254.

Caneva, G., Bartoli, F. Ceschin, S., Salvadori, O., Futagami, Y., Salvati, L., 2015. Exploring ecological relationships in the biodeterioration patterns of Angkor temples (Cambodia) along a forest canopy gradient. Journal of Cultural Heritage 16(5), 728-735.

Cappitelli, F., Zanardini, E., Sorlini, C., 2004. The biodeterioration of synthetic resins used in conservation. Macromolecular Bioscience 4(4), 399-406.

Charola, A.E., Delgado, R.J., Vale, A.M., 2008. Disfiguring biocolonization patterns after the application of water repellents. Restoration of Buildings and Monuments 14(5), 365–372.

Cutler, N.A., Viles, H.A., Ahmad, S., McCabe, S., Smith, B.J., 2013. Algal 'greening' and the conservation of stone heritage structures. Science of the Total Environment 442, 152–164.

Ettl, H., Gärtner, G., 1995. Syllabus der Boden-. Luft- und Flechtenalgen. pp. i-vii. 1-721. Stuttgart: Gustav Fischer.

Gambino, M., Sanmartín, P., Longoni, M., Villa, F., Mitchell, R., Cappitelli, F., 2019. Surface colour: an overlooked aspect in the study of cyanobacterial biofilm formation. Science of the Total Environment 659, 342-353.

Grondona, I., Monte, E., Rives, V., Vicente, M.A., 1997. Lichenized association between *Septonema tormes* sp. nov., a coccoid cyanobacterium, and a green alga with an unforeseen biopreservation effect of Villamayor sandstone at 'Casa Lis' of Salamanca, Spain. Mycological Research 101(12), 1489-1495.

Gorbushina, A.A., 2007. Life on the rocks. Environmental Microbiology 9, 1613–1631.

Guillitte, O., 1995. Bioreceptivity: a new concept for building ecology studies. Science of the Total Environment 167(1-3), 215-220.

Gustavs, L., Görs, M., Karsten, U., 2011. Polyol patterns in biofilm-forming aeroterrestrial green algae (Trebouxiophyceae, Chlorophyta). Journal of Phycology 47(3), 533-537.

Gustavs, L., Schumann, R., Karsten, U., Lorenz M., 2016. Mixotrophy in the terrestrial green alga *Apatococcus lobatus* (Trebouxiophyceae, Chlorophyta). Journal of Phycology 52, 311–314.

Häubner, N., Schumann, R., Karsten, U., 2006. Aeroterrestrial microalgae growing in biofilms on facades-response to temperature and water stress. Microbial Ecology 51(3), 285-93.

Houari, A., Seyer, D., Kecili, K., Heim, V., Di Martino, P., 2013. Kinetic development of biofilm on NF membranes at the Méry-sur-Oise plant, France. Biofouling 29, 109–118.

Knowles, E.J., Castenholz, R.W., 2008. Effect of exogenous extracellular polysaccharides on the desiccation and freezing tolerance of rock-inhabiting phototrophic microorganisms. FEMS Microbiology Ecology 66(2), 261-270.

Leelamanie, D.A.L., Karube, J., Yoshida, A., 2008. Characterizing water repellency indices: contact angle and water drop penetration time of hydrophobized sand. Soil Science and Plant Nutrition 54, 179-187.

Liu, X., Meng, H., Wang, Y., Katayama, Y., Gu, J.-D., 2018. Water is the critical factor to establishment biological and stability of Angkor temple sandstone in Southeast Asia. International Biodeterioration and Biodegradation 133, 9-16.

Macedo, M.F., Miller, A.Z., Dionísio, A., Saiz-Jimenez, C., 2009. Biodiversity of cyanobacteria and green algae on monuments in the Mediterranean Basin: an overview. Microbiology 155 (11), 3476-3490.

Madejová, J., Komadel, P., 2001. Baseline studies of the clay minerals society source clays: infrared methods. Clays and Clay Minerals 49(5), 410–432.

Mikhailyuk, T.I., 2013. Terrestrial algae from the granite outcrops of river valleys of the Ukraine. International journal on algae 15(4), 311-330.

Miller, A.Z., Sanmartín, P., Pereira-Pardo, L., Saiz-Jimenez, C., Dionísio, A., Macedo, M.F., Prieto, B., 2012. Bioreceptivity of building stones: a review. Science of the Total Environment 426, 1–12.

Moran, A.P., 2009. Microbial Glycobiology: Structures, Relevance and Applications. Elsevier, Oxford.

Martínez-Cortizas, A., Pérez-Alberti, A. (Eds.), 1999. Atlas climático de Galicia. Consellería de Medioambiente, Xunta de Galicia, 207p.

Nugari, M.P., Pietrini, A.M., Caneva, G., Imperi, F., Visca, P., 2009. Biodeterioration of mural paintings in a rocky habitat: the Crypt of the Original Sin (Matera, Italy). International Biodeterioration and Biodegradation 63, 705-711.

Ortega-Calvo, J.J., Ariño, X., Hernandez-Marine, M., Saiz-Jimenez, C., 1995. Factors affecting the weathering and colonization of monuments by phototrophic microorganisms. Science of the Total Environment 167, 329-341.

Pfendler, S., Munch, T., Bousta, F., Alaoui-Sosse, L., Aleya, L., Alaoui-Sossé, B., 2018. Bleaching of biofilm-forming algae induced by UV-C treatment: a preliminary study on chlorophyll degradation and its optimization for an application on cultural heritage. Environmental Science and Pollution Research 25(14), 14097-14105.

Pinna, D., 2017. Coping with biological growth on stone heritage objects: methods, products, applications, and perspectives. Apple Academic Press, Toronto.

Polson, E.J., Buckman, J., Bowen, D.G., Todd, A.C., Gow, M.M., Cuthbert, S.J., 2002. Biofilms on porous building materials: friend or foe? In 9th International Conference on Durability of Building Materials and Components.

Pozo-Antonio, J.S., Rivas, T., Carrera, F., García, L., 2018. Deterioration processes affecting prehistoric rock art engravings in granite in NW Spain. Earth Surface Processes and Landforms 43, 2435-2448.

Rifón Lastra, A., 2000. Algas epilíticas en monumentos de interés históricos de Galicia. PhD thesis, Universidade de A Coruña, Spain.

Rifón Lastra, A., Noguerol Seoane, A., 2001. Green algae associated with the granite walls of monuments in Galicia (NW Spain). Cryptogamie, Algologie 22 (3), 305-326.

Rindi, F., Guiry, M.D., 2004. Composition and spatial variability of terrestrial algal assemblages occurring at the bases of urban walls in Europe. Phycologia 43, 225-235.

RILEM (Reunion Internationale des Laboratoires d'Essais et de Recherche sur les Materiaux et les Constructions). 1980. Commission 25 PEM. Protection et Erosiondes Monuments. Recommandations provisoires. Essais recommandes pour mesurer l'alteration des pierres et evaluer l'efficacite des methodes de traitement [French]. Test No. II. 1: Open porosity and Test II. 2: Bulk and real densities.

Rivas, T., 1997. Mecanismos de alteración de rocas graníticas utilizadas en la construcción de edificios antiguos de Galicia. PhD thesis, Universidade de Santiago de Compostela, Spain.

Rivas, T., Prieto, B., Silva, B., 2000. Influence of rift and bedding plane on the physico-mechanical properties of granitic rocks. Implications for the deterioration of granitic monuments. Building and Environment 35, 387-396.

Rueden, C.T., Schindelin, J., Hiner, M.C., DeZonia, B.E., Walter, A.E., Eliceiri, K.W., 2017. ImageJ2: ImageJ for the Next Generation of Scientific Image Data. BMC Bioinformatics 18, 529.

Sanmartín, P., Rodríguez, A., Aguiar, U., Medium-term field evaluation of several widely used cleaning-restoration techniques applied to ~~phototrophic~~ algal biofilm formed on a granite-built historical monument. International Biodeterioration and Biodegradation, this issue.

Sanmartín, P., Fuentes, E., Montojo, C., Barreiro, P., Paz-Bermudez, G., Prieto, B., 2019. Tertiary bioreceptivity of schists from prehistoric rock art sites in the Côa Valley (Portugal) and Siega Verde (Spain) Archaeological Parks: effects of cleaning treatments. International Biodeterioration and Biodegradation 142, 151-159.

Silva, B., Sanmartín, P., Prieto, B., 2019. Characterization of the support rock of the petroglyphs of Campo Lameiro (Pontevedra). Cadernos do Laboratorio Xeolóxico de Laxe vol. 41 (In Spanish). ISSN: 0213-4497.

Socrates, G., 2001. Infrared and Raman Characteristic Group Frequencies: Tables and Charts, 3rd edn. John Wiley & Sons: Baffins Lane, Chichester.

Steffgen, T., 2019. Experimental studies - Building physics investigations in condensation water on plaster surfaces Pollack Periodica 14(1), 167-175.

Thornbush, M.J., 2013. Digital Photography Used to Quantify the Greening of North-Facing Walls along Broad Street in Central Oxford, UK. Royaume-Uni. Geomorphologie: Relief, Processus, Environment 2, 111-118.

Thornbush, M.J., 2014. Orientational Effects on Soiling Measurements at the Sheldonian Theatre in Central Oxford, UK. Journal of Buildings Research, Conscientia Beam, vol. 1(1), 1-27.

UNE-EN 1936:1999. Natural stone test methods, Determination of real density and apparent density, and of total and open porosity, AENOR (Spanish Association for Standardisation and Certication).

Vázquez-Nion, D., Silva, B., Prieto, B., 2018. Influence of the properties of granitic rocks on their bioreceptivity to subaerial phototrophic biofilms. Science of the Total Environment 610–611, 44–54.

Viles, H., Ahmad, H., 2016. Architectural controls on the bioreceptivity of sandstone to green algal colonization. ECBSM2016. European Conference on Biodeterioration of Stone Monuments - Second Edition. Cergy-Pontoise, France. November 17–18, 2016.

Villa, F., Remelli, W., Forlani, F., Gambino, M., Landini, P., Cappitelli, F., 2012. Effects of chronic sub-lethal oxidative stress on biofilm formation by *Azotobacter vinelandii*. Biofouling 28, 823–833.

Villa, F., Pitts, V., Lauchnor, E., Cappitelli, F., Stewart, P.S., 2015. Development of a Laboratory Model of a Phototroph-Heterotroph Mixed-Species Biofilm at the Stone/Air Interface. Frontiers in Microbiology 6, 1251.

Vojtková, H., 2017. Algae and their biodegradation effects on building materials in the Ostrava industrial agglomeration IOP Conference Series: Earth and Environmental Science. 92(1), 012073.

Wurtz, A., 1944. Remarques sur une Pleurococcacée: *Apatococcus vulgaris* Brand. Bulletin de la Société Botanique de France 91 (7/8), 185-190.

XLSTAT 2019: Data Analysis and Statistical Solution for Microsoft Excel. Addinsof, Paris, France.

Zhang, G., Gong, C., Gu, J., Katamaya, Y., Gu, J.-D., 2019. Biodeterioration and the mechanisms involved of sandstone monuments of World Cultural Heritage sites in tropical regions. International Biodeterioration and Biodegradation 143, 104723.

Figure legends

Figure 1. The four background walls of the processional cloister of the Monastery of San Martiño Pinario. N: north-facing wall, S: south-facing wall, E: east-facing wall, W: west-facing wall.

Figure 2. Confocal laser scanning imaging of the ~~the~~ biofilm~~-~~ collected from the most hydrophobic areas~~on the stone surfaces~~. Colour key~~ for panel A~~: phototrophs, blue (autofluorescence); total chemotrophs, green (Syto9); extracellular glycoconjugates, red (Con A); stone, grey (reflection). Scale bars are 100 µm.

Figure 3. (A) General appearance of the biofilm, with drops of water suspended after moistening, photographed with a digital camera. (B) Detail of the moistened biofilm, photographed with a digital microscope (Dino-Lite AM3113T). (C) *Apatococcus lobatus* cell morphology observed under a light microscope (Nikon Eclipse 50i). Scale bar = 50 µm (B); 5 µm (C). ~~(scale = 5 µm).~~

Figure 4. Contact angle (degree) and WDPT: water drop penetration time (s). Photographs and microphotographs of samples with (A.1) biofilm with highest water repellency, (A.2) biofilm with lowest water repellency, (B) granite surface after removal of the biofilm, (C) algal cells without the extracellular matrix on a nitrocellulose membrane, (D) nitrocellulose membrane. Water repellency categories according to Leelamanie et al. (2008).
Asterisk indicates that measurements were made immediately after placing the drop of water on the surface.
3 s and 10 s: Photographs taken 3 and 10 seconds after placing the drop of water on the surface.

Figure 5. Photographs of fragments of samples from background walls of the processional cloister. A-B) Uncolonized granite surface; C-E) Colonized granite surface with *A. lobatus* algal biofilm; F) Detail of *A. lobatus* sarcinoid aggregrates. Scale bar = 150 µm (A, B); 250 µm (C); 100 µm (D, E); 25 µm (F).

Figure S1. Arch in the central courtyard with the pattern outlined by the biofilm growth and sunlight projecting on the background walls of the processional cloister.

Figure S2. Box plots of the EPS components. A) Polysaccharide content (micrograms per milligrams of the total biomass of the biofilm). Asterisk above the whisker indicates significant difference between means according to the Mann–Whitney U-test (U = 34.0; p-value = 0.009) performed after that Kruskal Wallis test showed significant differences between 1 - 2 and 3 – 4 (H = 6.987; p-value = 0.075). B) Protein content (μg per mg of the total biomass of the biofilm), Kruskal-Wallis test showed no significant difference (H = 3.101; p-value = 0.376).

Figure S3. Correlation between EPS components and the contact angle values. The strength of linear relationship between paired data is indicated by Pearson's correlation coefficient (R) and t test of the regression slope (significant at $p < 0.05$).

Figure S4. ATR-FTIR spectra obtained from the granite samples from uncolonized adjacent areas (N1-N3) and from underneath the biofilm (U1-U3). Y-axis: absorbance (A.U.). X-axis: wavenumber (cm^{-1}).

Video S1. Water repellency of *A. lobatus* subaerial biofilm.

Table S1. Semi-quantitative XRD data for the granite samples from adjacent uncolonized areas (N1-N3) and from underneath the biofilm (U1-U3).

Sample	Component (wt.%)					
	Quartz	Plagioclase	Microcline	Mica(*)	Chlorite	Gypsum
N1	30	23	13	20	5	9
N2	31	19	21	17	3	8
N3	49	16	13	17	5	-
U1	44	12	22	20	2	-
U2	39	24	17	17	4	-
U3	48	13	19	16	1	-

(*) Muscovite and Biotite.